**Twin Tests
Book of Reference**

Twin Test 1: Effects of Vegetation on Flows in the Urban Environment

Lead Beneficiary: KIT
Dissemination Level: Public

Authors: V. Pappa, N-P Pallas, D. Bouris, C.Gromke, V. Riziotis, M. Manolesos, J. Prospathopoulos, P. Chasapogiannis, K. Kellaris , K. Vassilopoulos

Deliverable 4.1

WP4

Widening of technical capacity and competence

Executive Summary

The present chapter of the book of references refers to the first twin test of the TWEET-IE project, carried out in the wind tunnels of the Karlsruhe Institute of Technology and the National Technical University of Athens. An investigation of the effects of vegetation on flow in the urban environment is carried out through the study of the flow past a cube shaped building exposed to an atmospheric boundary layer. The building has openings on its side (with respect to the oncoming flow) walls. Identically shaped buildings were studied in both wind tunnels and efforts were made to well document their similar upstream atmospheric boundary layers in terms of both mean velocity, turbulence intensity and integral length scales. The study at KIT was performed with a Laser Doppler Velocimetry (LDV) System and at NTUA with a 2D-3C Particle Image Velocimetry (PIV) system. The beginning of the report documents details of the measurement methods and practical advice resulting from their application during the experiments at the two different wind tunnels. Comparison of the two measurements is then presented at the same relative positions around the cube. Furthermore, simulated vegetation was placed on the upstream face and on the roof of the building and its effects were studied, again in both wind tunnels. Results and analysis of the measurements are presented. Overall, qualitative trends agree well between the two measurements and the same effect of vegetation is found in both measurement sets. Results are not quantitatively identical but their differences provide an opportunity to analyse the effects of the different upstream conditions, wind tunnel configurations and measurement techniques.

History and Changes

Ver	Date	Description	Contributors
1.0	30/10/2023	Report	KIT, NTUA
1.1	17/11/2023	Minor corrections	KIT, NTUA

Contents

List of figures

List of tables

1 Introduction

The scope of the test and methods presented in the present chapter is twofold:

1) In the context of the TWEET-IE project, a twin test is performed. One wind tunnel testing campaign is performed in the wind tunnel at Karlsruhe Institute of Technology (KIT), Germany and a second test is performed at the National Technical University of Athens (NTUA), Greece.

   The experimental setup is the same in both tests: a cube shaped building model is exposed to a boundary layer flow. The building has vertical openings on its side faces, with respect to the flow direction, and its roof and front face are alternately covered with foam material, intended to simulate vegetation (*Figure 1*). Although the wind tunnels are of different cross section, care is taken to preserve Reynolds number independence, to achieve the same upstream boundary layer (simulating the same atmospheric boundary layer conditions) and the same conditions of velocity and turbulence.

   Measurements of velocity and turbulence quantities are performed using hot wire anemometry, in both wind tunnels, for documenting the upstream boundary layer. For the flow around the building model, point measurements of two velocity components are performed using Laser Doppler Anemometry (LDA) at KIT and planar measurements of two and three velocity components are performed using Particle Image Velocimetry (PIV and Stereo PIV) at NTUA.

   Measurement space overlaps among the two tests and so comparison of the results is possible to identify, characterize and categorize important sources (external conditions, testing equipment etc.) of deviations between test data obtained at different tunnels

2) The tests are of significant research value in themselves as they examine the effects of vegetation, included on the surfaces of buildings, on the flow around the buildings and through the openings. These effects are of relevance both to the wind flow in the urban environment, affecting pedestrian comfort and air quality, as well as to indoor air quality. The dependence and relation of indoor air quality and the natural ventilation potential of a building to the presence of vegetation on its outer surfaces is a current subject of research.

Figure 1 Cube shaped building with vertical openings in boundary layer wind tunnel. Left: cube without vegetation (bare); Middle cube with façade greening at the windward wall; Right: cube with roof greening.

The current report presents the methods, materials, procedures and results of the twin tests carried out at KIT and NTUA. The level of detail is not intended to substitute manuals or equipment specific information. It is rather a documentation of procedures followed and experience gained through the tests, in order to

   a) facilitate cross comparison of the results

b) facilitate assessment of sources of deviations among the "twin" tests, in order to ultimately improve procedures
c) provide a starting point for users of the facilities
d) provide a guide for researchers intending to perform similar tests

2   KIT - Equipment and Methods. Training and Documentation

2.1 Introduction

2.1.1 The wind tunnel at KIT

The Wind Tunnel (WT) is at the Laboratory of Building and Environmental Aerodynamics which is a research group at the Institute for Hydromechanics (IfH) of the Karlsruhe Institute of Technology (KIT). It is a low speed (subsonic) semi-open circuit WT, powered by a 35 kW motor with a total length of ≈ 9 m and a closed test section of (w)x(h)x(l): 2x1x2 m. The WT is operated as a neutrally stratified atmospheric boundary layer wind tunnel with a maximum free-stream velocity of 20 m/s (*Figure 2*). Further details on the Wind Tunnel setup and characteristics of the simulated atmospheric boundary layer flow can be found in Chapters 4.1.1 and 4.1.3, respectively.
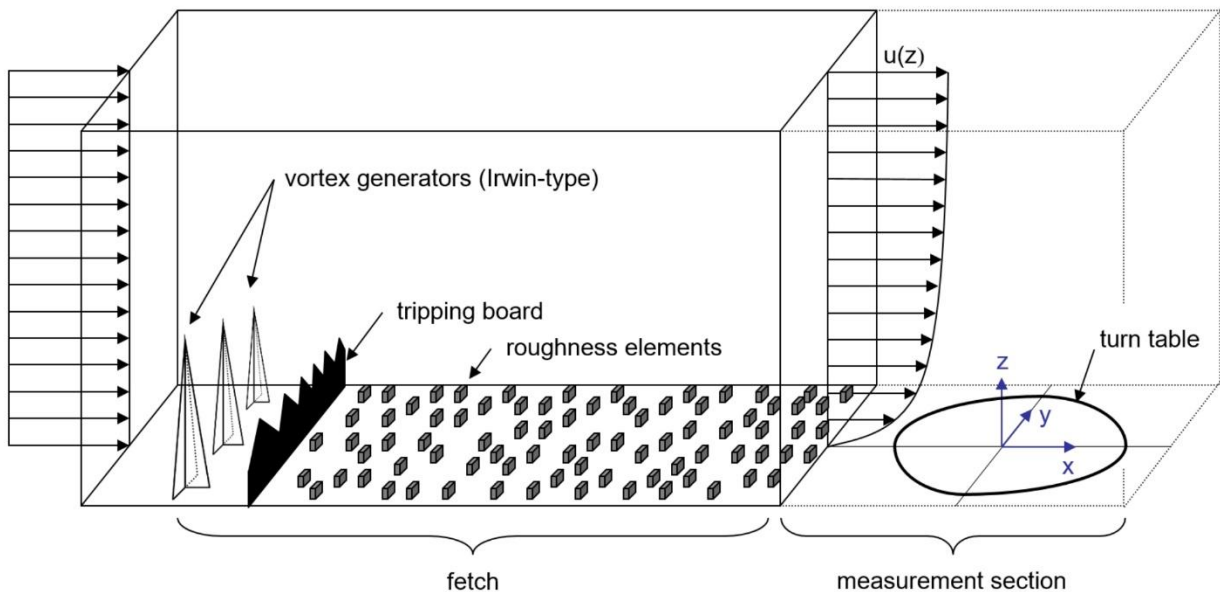
Figure 2 Atmospheric boundary layer (ABL) Wind Tunnel layout

The fetch and measurement section features:

- An electrically powered turntable to allow orientation of the model with the flow at a specified angle.
- An electrically powered 3D traversing system to position measurement instrumentation.
- A transparent sidewall (one-sided) for optical access of the WT by the user and measurement instrumentation (e.g. laser-based flow measurement techniques, cameras).
- Spires (Irwin-type vortex generators), ground-mounted tripping board, and roughness elements for creating a simulated atmospheric boundary layer with characteristics (friction velocity, roughness length, turbulence length scales) that allow a simulation scale of 1:100 - 300.

2.1.2 LDV instrumentation

This section provides a short description of the employed LDV measurement system and of related equipment and its implementation / integration specific to the WT at the Laboratory of Building and Environmental Aerodynamics. For the theory and working principle of LDV the reader is referred to e.g. [1],[2],[3],[4].

A 2-component dual-beam LDV system operating in the backscattering mode from TSI was employed. The system consisted of a nominal 4W continuous wave (cw) argon ion laser (type Innova 70, Coherent). It is noted that the argon ion laser was serviced 2 to 3 months before the measurement campaign. The service involved among others refilling of the tube with lasing gas. As a result, the maximum available laser output power was somewhat higher than 4W at the beginning of the measurement campaign and slightly lower than 4W at the end of the measurement campaign, as measured on-site with a laser power meter. Upon color separation of green (514.5 nm) and blue (488.0 nm) followed by beam splitting and frequency shifting of one partial beam of each color in a multicolor beam separator (type Model 9201 ColorBurst, TSI), the beams were coupled by means of fiber-optic couplers (type Model 9271, TSI) into a fiber-optic (type Model 9800 Series, TSI). The fiber-optic ensures safe transmission of the laser light to a remote position where a probe head (Model 9251-102) serving as emitting and receiving optic is located (*Figure 3*). The probe head has a cylindrical shape of length 180.3 mm and diameter 25 mm. With a lens focal length of 110.3 mm and a beam-crossing half angle of 3.9° spheroid measurement volumes were created. The nominal dimensions and characteristics of the measurement volumes for the two colors based on the $1/e^2$ intensity criterion reduction were:

- green (514.5 nm): length 1.1 mm, max. diameter 73.4 μm, 19 fringes, fringe spacing 3.78 μm,
- blue (488.0 nm): length 1.0 mm, max. diameter 69.6 μm, 19 fringes, fringe spacing 3.59 μm.
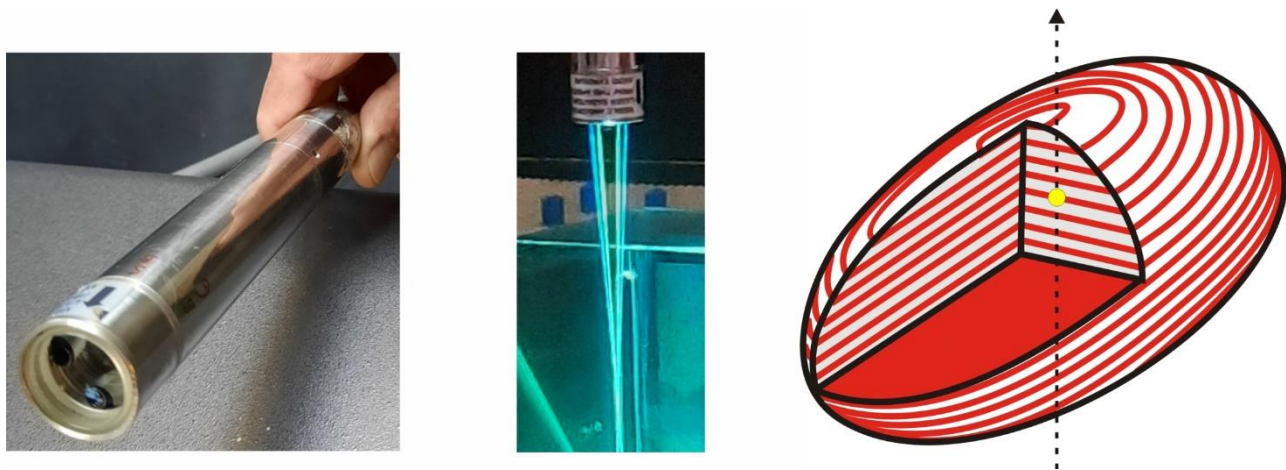
Figure 3 Probe head, emitted laser beams, and illustration of spheroid measurement volume

The backscattered light was converted to electrical signals by a multicolor receiver / transducer (type Model 9230 ColorLink Plus, TSI). Following this step, the electrical outputs were processed by a digital signal processor (type Model FSA3500, TSI). Specific to the LDV system setup at KIT was that the multicolor receiver / transducer was controlled by a PC with operating system Windows 98 whereas the digital signal processor was controlled by a PC with operating system Windows 7. The measurement settings and data acquisition were performed using the

software FlowSizer64 from TSI. In addition to the installations described above, the output signals from the multicolor receiver / transducer were displayed on an oscilloscope to allow for an independent visual on-line check of the LDV bursts and for an assessment of the plausibility / reliability of the measurements.

2.1.3 Seeding

A very important aspect in LDV are the seed particles. LDV acquires the motion of the seed particles which are considered being representative of the motion of the fluid. Hence, seed particles should theoretically ideally follow the flow. The particle following behavior is characterized by the Stokes number St. A small Stokes number (St << 1) indicates a good particle following behavior.

For the current measurements, two methods to generate seed particles were utilized, one for LDV of the flow around / outside the cube (exterior flow), and a second for LDV of the flow inside the cube (interior flow). For LDV of the exterior flow, the seed particles were generated by the vaporization and subsequent condensation of a custom-made fog fluid consisting of propylene glycol (80%) and distilled water (20%). A fog machine (type F48 Fog Machine) was used to generate the seed particles. This process resulted in seed particles of diameter 1-3 μm which persisted for O(10 sec) in the flow before evaporating and having an adequate following behavior [5]. It is noted that also another fog generator in combination with the same liquid mixture was employed (type Captain D, Smoke Factory) with which, however, significantly lower LDV signal rates were obtained.

For LDV of the interior flow, the seed particles were generated by vaporization and subsequent condensation of a commercial fog fluid (type Heavy Fog, Smoke Factory). The seed particles were produced in a custom-made fog machine which consisted of a cylindrical tank whose bottom was covered by a layer of 1-2 cm fog fluid. Tube-shaped ceramic heating elements (type 501, Seuthe) with a capillary tube at their lower end were partially immersed in the fog fluid and produced the seed particles (*Figure 4*). The tank was supplied with a controlled volume flow rate of air which transported the seed particles via a tubing system to a plenum chamber below the cube. In order to realize a spatially and temporally reasonably homogenous and non-intrusive supply of the cube with seed particles, the cube bottom plate was perforated by a regular array of circular openings constituting an area source. The openings were connected by hypodermic needles of 40 mm length and 0.57 mm inner diameter to a plenum chamber below the cube (*Figure 4*). It is noted that the area source modelling followed the approach described in [6] for line sources.
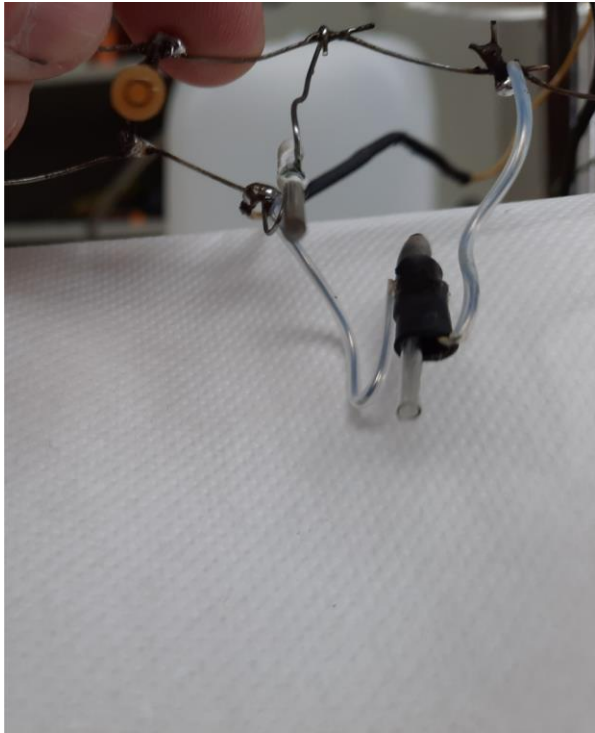
Figure 4 Ceramic heating elements and area source in cube bottom with hypodermic needles and plenum chamber.

2.1.4 Laser safety

Depending on their output power, lasers are classified. Lasers typically employed in LDV fall into the highest laser class, which is class 4 ($\geq$ 500 mW). The power of class 4 lasers can burn skin or induce skin damage and cause eye damage. It is important to realize that also scattered light from class 4 lasers can cause skin and eye damage. Hence, highest precaution and safety measures are mandatory when performing LDV.

At the Laboratory of Building and Environmental Aerodynamics, every person working with the LDV system must complete a laser safety instruction before using it for the first time. The laser safety instruction is given by the laser safety officer of the Institute for Hydromechanics (IfH). Scope and content of the laser safety instruction can be taken from guidelines of published employers' liability insurance associations. It should be noted that country-specific there may be various employers' liability insurance associations that deal with laser safety issues. Hence, no further references are provided here. Instead the reader is called upon to take care of it himself depending on geographic location and employers' association allocation.

Moreover, next to the basic and general laser safety rules / instructions as provided by the employers' liability insurance associations, the implementation of laser safety measures is site (laboratory) and experiment setup / conditions specific. Prior to each new experiment setup careful considerations targeted to the specific conditions must be done. A detailed example of site and experiment specific laser safety measures / instructions is given for the NTUA wind tunnel environment in Chapter 3.1.3.

2.2 Test preparation

2.2.1 Model preparation

The aim of the experiments performed in the atmospheric boundary layer wind tunnel at KIT was to acquire the flow field around and inside the cube for various wall (windward wall) and roof vegetation scenarios by means of LDV (*Figure 5*). In particular, the measurement of the interior flow poses special requirements on the provision of seed particles inside the cube and on the cube material. The generation of seed particles for LDV of the interior flow and their delivery to the inside cube via an area source involving a plenum chamber and hypodermic needles was already addressed in Chapter 2.1.3. The therein described approach was specially conceived and developed for the current experiments and proved to be viable. In order to allow for LDV inside the cube, the cube material has to be transparent for light in the visible wavelength range. It was chosen to make the cube of glass with layer thickness 5 mm instead of the commonly for wind tunnel models utilized perspex. The reason was that perspex is much more prone to surface scratches than glass. Those can result as a consequence of cleaning processes that are regularly necessary since seed particles (fog) deposit on the cube surfaces and detrimentally affect the LDV signal quality and rate. In order to allow for a cleaning of the inside-facing cube walls, the top glass plate (roof) was made removable.
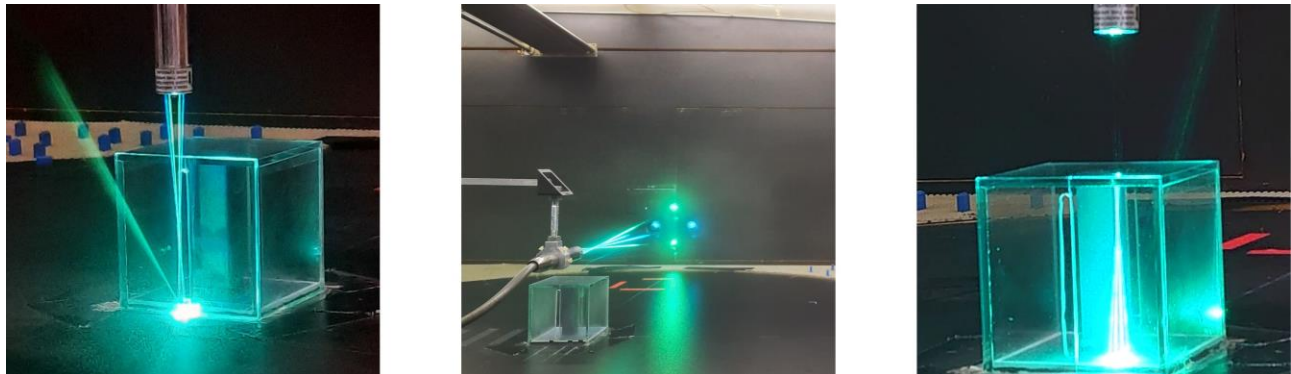
Figure 5 Two-component LDV at the glass cube in the atmospheric boundary layer wind tunnel at KIT. Left: outside the cube in front of a vertical opening; Middle: outside above the cube roof; Right: inside the cube.

Façade and roof vegetation was modelled by a layer of porous foam, which was attached to the corresponding surface. The presentation of the modelling and scaling criteria for representing vegetation in reduced scale wind tunnel experiments goes beyond the scope of the current report. For a detailed description of the modelling approach, the reader is referred to [7,8]. For details of the geometry of the cube, of the vertical openings, and the type of vegetation and its positioning at the cube, the reader is referred to Chapter 4.2 of this report.

2.3 Quality Assurance

2.3.1 LDV measurements

2.3.1.1 *Release of seed particles for LDV of flow around / outside the cube (exterior flow)*

The LDV measurements of the exterior flow rely on the presence of seed particles in the outside surrounding of the cube. To allow for velocity times series with equidistant time step and moreover for equivalent conditions in the entire measurement field, a continuous (in time) and spatially uniform distribution of seed particles is required. In the current experiment setup, the seed particles were released from a hole (approx. 5 cm diameter) flush mounted to the wind tunnel floor and located approx. 4 m windward of the cube. This arrangement ensured that the initially, upon release from the floor hole, meandering plume of seed particles was sufficiently dispersed in the measurement field around the cube and exhibited a continuous and homogenous distribution.

2.3.1.2 *Release of seed particles for LDV of flow inside the cube (interior flow)*

The realization of the area source in the cube for the release of seed particles for the LDV of the interior flow was already described before, see Chapter 2.1.3.

2.3.1.3 *Positioning of the LDV measurement volume*

In flows with larger velocity gradients, e.g. in a boundary layer close to a wall, the knowledge and control of the position of the measurement location is as important as the accuracy of the measurement technique itself.

The laser probe head (*Figure 3*) is moved by a 3-axis custom-made traverse system controlled by a PC. At the beginning of the measurement along a traversing profile, the position of the LDV measurement volume was determined by means of a target plate, which was made coincident to intersection of the laser beams (measurement volume). In addition, during the course of a measurement along a traversing profile, the actual position of the measurement volume was regularly checked.

2.3.1.4 *LDV control and acquisition settings*

The following main / basic settings were chosen for the 2-component LDV:
- Bragg cells enabled to generate frequency shifts in each of the components in order to allow for the detection of flow reversals.
- Even time sampling enabled to obtain time series of defined nominal uniform sampling frequency.
- Coincidence mode enabled to ensure the simultaneous acquisition of the two components based on the defined nominal coincidence time.

Prior to the recording at a certain measurement location, the photomultiplier voltages, the burst thresholds, and the filter band widths were adapted in an online screening such that plausible velocity data at a rate complying with the targeted sampling frequency were obtained.

Further information on the realized acquisition settings in the actual measurements (e.g. sampling frequency, measurement duration etc) are provided in the description of the experimental configurations in Chapter 4.2.1.

2.3.2 Wind Tunnel approach flow

2.3.2.1 ABL characterisation

Details on characteristics of the simulated atmospheric boundary layer approach flow are given in Chapters 4.1.1 and 4.1.3.

2.3.2.2 Flow Symmetry

Although wind tunnels are usually designed and constructed such that a flow symmetric to the streamwise vertical central plane should exist, the actual prevailing flow exhibits deviations from symmetry. This is due to small imperfections which are not under the control of the wind tunnel designer or operator.

In order to ensure that the flow is as symmetrical as possible around the cube in the current experiments, pre-tests were carried out. To this end, the turntable with the cube in the center of the measurement section of the wind tunnel was slightly rotated in an angular range close around its nominal 0° position and LDV of the lateral flow component in front of the vertical opening at both freestream-parallel sidewalls were performed. Based on these pre-tests, the turntable was rotated by 1° in anti-clockwise direction for the following measurement series.

3 NTUA - Equipment and methods. Applied Knowledge.

3.1 Introduction

3.1.1 The NTUA wind tunnel

The NTUA WT facility is under the Fluids Section of the School of Mechanical Engineering and is used by the Laboratory of Aerodynamics and the Laboratory of Innovative Environmental Technologies. It is a low speed (subsonic) closed circuit WT, with an 8 bladed axial fan, powered by a 350hp motor. It has a total length of ~70 m with 3 test sections of (w)x(h)x(l): 1.8x1.4x3.2 m, 3.5x2.5x12.1 m, 4.5x3.5x3.5 m. The present test was performed in the 3.5x2.5x12.1 m test section (*Figure 6*).

Figure 6 Wind Tunnel layout

The test section includes:
- An electrically powered rotating floor, to allow orientation of the model with the flow at a specified angle
- An electrically powered and electronically controlled 3D traversing system, to position a measurement device (e.g. hot wire anemometer, Pitot tube) at a desired position in the flow
- Transparent side walls for optical access of the WT user and the instruments (e.g. lasers, cameras)
- A maximum attainable free stream velocity of ~10 m/s when passive ABL generation devices are installed
- Turbulence generating screens for a minimum attainable free stream turbulence level of 2%
- Spires and roughness elements for creating a simulated atmospheric boundary level with characteristics (friction velocity, roughness length, turbulence length scales) that allow a simulation scale of 1:200-300.

3.1.2 PIV measurements

In this section, a brief description of the fundamentals of Particle Image Velocimetry, the equipment available at NTUA is presented for completeness. Emphasis is placed on the use of all the components of the PIV system as well as the communication/interconnection between them.

Particle Image Velocimetry (PIV) is based on the principle of optical tracking of particles, whose trajectories and velocities are considered to represent those of the fluid flow. Having started the motor of the wind tunnel, seeding particles are injected in the test section through an appropriate opening. For the production of the seeding particles, a system of compressed air (Figure 7) may be required, consisting of a compressor and an appropriate tubing system leading the compressed air to the droplet generator (**Error! Reference source not found.**) located in the control room of the wind tunnel. A high-energy laser (connected to a cooling system, see Figure 9) as well as at least one PIV camera (i.e. high-speed camera, see Figure 10) are required. For the acquisition of 2 component (2C) velocity measurements on a specific plane (2D) of interest, only one high-speed camera is prerequisite (2D/2C PIV) while for 3 component (3C) planar (2D) velocity measurements two high-speed cameras are necessary, in order to obtain a perspective of depth (2D/3C or Stereo-PIV). For the undertaking of 3-D volumetric measurements, at least 3 high-speed cameras have to be present to capture the 3 component (3C) velocity field in a desired volume (3D), similar to 3D tomography, instead of a single plane of interest (3D/3C or tomo PIV). In the present test, only Mono (2D/2C) PIV as well as Stereo (2D/3C) PIV will be the topics of interest.

The employed laser produces a pulsating laser sheet which illuminates the plane of interest. The camera (or cameras if applicable), being synchronised with the pulse of the laser, obtains two consecutive frames (frame A and frame B, comprising one PIV snapshot/recording) which are then sent to a computer for further processing. The obtained consecutive frames are divided into sub-regions (interrogation windows) where each sub-region contains a number of illuminated seeding particles. Of course the seeding particles have moved due to the fluid motion, so their initial position in frame A is different from that of frame B. The reflection of the illumination (produced by the laser) on the injected particles and the subsequent light scattering is the key component of the PIV technique. More specifically, most often by means of cross-correlation, the displacement distance of the seeding particles is identified, and therefore, the velocity of the seeding particles can be calculated by considering the time between the two frames (pulse separation time). Finally, with the assumption that the flow patterns are accurately reproduced by the seeding particles, the planar velocity field is acquired. For the synchronisation between the high-speed camera(s) and the pulse of the laser (determined by the pulse separation time), a synchroniser (see Figure 11) is necessary. This synchronisation can be also ensured by a computer via a specific software (e.g. INSIGHT 3G by TSI Instruments). It is noted that due to optical access problems, the utilisation of reflectors (mirrors) leading the laser sheet to the area of interest, may be required. Finally, velocity vectors are extracted from the captured images (raw data) by an appropriate software [9].

Note that there are numerous other configurations for both Mono and Stereo-PIV (e.g. in terms of exposure, camera sensors, seeding particles, laser equipment etc.) but those described here are most relevant to what has been applied during the present measurements.

Figure 7 Compressed air system (Shultzer)

Figure 8 Droplet generator (TSI model 9307

Figure 9 Laser apparatus (LYTRON 200 mj Nd:YAG)

Figure 10 High-speed PIV camera (TSI PowerViewPlus 4MP)

Figure 11 *Synchroniser (TSI 610034)*

The majority of the above-mentioned components are usually provided as a complete PIV system (laser + cameras + synchroniser + computer + installed software + other elements e.g. protective goggles, calibration target etc.). The manual to this system provides detailed information on its operating principles and procedures while in depth understanding of the PIV methodology can be acquired from textbooks. There is also the option to build a PIV system "from scratch" by acquiring separately all the necessary components.

Complementary measurements may be required (e.g. pressure measurements via pressure taps, velocity measurements through hot-wire anemometry) to determine the atmospheric boundary layer - ABL profile and the reference velocity, *Re* number etc.

3.1.3 Laser Safety Instructions

The PIV system operation relies on the utilization of a laser light source, whose energy may be dangerous without proper precautions. In this section, basic safety instructions regarding the operation/handling of the equipment comprising the experimental apparatus will be given (a) for the protection of the user and other personnel in the vicinity of the facility and (b) for the protection of the equipment. General instructions are as follows:

- All components of the experimental apparatus have to be in a secured position i.e. the laser, the camera(s) etc. have to be firmly fastened and/or fixed to a solid surface.
- It has to be ensured that there is enough coolant inside the laser apparatus at all times. This requires frequent check of the temperature of the laser system.
- It is strongly advised to restrict the space occupied by expensive equipment (e.g. the laser apparatus) with safety tape.
- Unsupervised operation of the wind tunnel and the equipment must be avoided
- During the experiment, access must be restricted and controlled. Only trained personnel, contributing to the experiment should be present, in order to minimise the possibility of an accident.
- If inexperienced laboratory staff are present, they must follow the instructions of the more experienced experimentalists.
- Extreme caution is required during the operation of the system of air compression. All limits referring to temperature or pressure (e.g. temperature of the motor, oil pressure etc.) have to be monitored and complied with.
- In case of fatigue, the experimentalists should immediately stop operating the wind tunnel and the experimental equipment or seek assistance.
- After the experiment, a final check of all the equipment should be performed. It has to be ensured that all electric devices are turned off as well as that the employed pneumatic systems (compressor, droplet generator etc.) and the wind tunnel are not in operation.

The laser may be considered as the most dangerous component for the end user and also the most expensive. The following operational measures have to be strictly followed when working with lasers [10]

➢ Before the laser is turned on:
  1. Take off all worn reflective objects (jewelry, watches,...).
  2. Make sure no object is in the path between the laser head up to the measurement part (usually a slice), except the optical components to control the laser beam.
  3. Verify that all protective measures are in place, in particular curtains and warning signs on doors.
  4. Turn on the gyro-flash lights.
  5. Close doors.
  6. Put on laser safety goggles.

7. With cameras: close camera lens with protective cover and set aperture to minimum (closing), i.e. highest f number.

➢ Turning the laser on:
1. Verify that all points above are assured - go systematically through them (check-list).
2. Inform others loud and clearly that you are about to turn the laser on. Wait for their "OK" before actually turning on the laser.
3. Stand in safe position, outside of path and curtains.
4. Turn on with minimum power.

➢ When the laser is on:
1. Avoid abrupt movements and limit movements around the laser.
2. Never take the goggles off.
3. Never make any modifications to optical set-up or anything else with laser on.
4. Cameras: display live images, take of lens cover, check for possible satura-tions and then only proceed to decrease f number. Remember, when refocus-sing, high light intensities can occur.

➢ After turning off laser:
1. Take off goggles: put them back into their case.
2. Turn off gyro-flash lights.

➢ General security rules, set-up:
1. Cover beams as much as possible.
2. NEVER have eyes at beam level, even when you think that the laser is shut/off.
3. Protect rather than close eyes. Closed eyes are unsafe. Many accidents when working with lasers are not related to laser radiation but with the fact that people bruise their fingers or trip, sometimes as a result of limited vision when wearing laser safety goggles.
4. Block beam before handling optical elements or using reflective tools.
5. Block all spots and reflections leaving your set-up / not being used.
6. Never use reflective tools.
7. Place computer screens out of beam height or shield them.

Even following these measures strictly does not guarantee 100% safety. 100% safety is impossible. Do all you can to reduce accidents to a minimum. It is noted that the employed Nd:YAG Laser used in this application, apart from potentially causing permanent eye damage, has enough energy to burn skin or combustible materials. [1]

---

[1] Disclaimer: these are safety measures specific to the NTUA lab. Although similarities with the measures necessary for other labs may occur, they are by no means exhaustive or sufficient and additional / further specific safety measure may be required in other labs.

3.2 Test Preparation

3.2.1 Model Preparation

A key component of every wind tunnel test is the preparation of a suitable model corresponding to the particular needs of the experiment that is to be conducted. This includes:

- Suitable choice of the model material for minimal roughness, optical access (glass or plexiglass), durability (scratches) etc. For PIV applications, this should minimize reflections, otherwise the captured images will be contaminated by unwanted noise. If, for any other reason, the chosen material is such that reflections cannot be completely avoided, other measures have to be taken e.g. using non-reflecting paint or other substances such as Rhodamine fluorescent paint. This was the case in the framework of the current experiment, whereby the plexiglass cube was painted with black non-reflective paint.

- If surface pressure measurements are also required, additional care has to be taken to ensure that appropriate pressure taps are mounted onto the surfaces of interest. This is not always a trivial task, especially if complex geometries are implicated. The employed cube for the presented wind tunnel experiment offers the opportunity of surface pressure measurements via installed pressure taps on its roof and façade. These pressure taps are connected through an appropriate tubing system to a pressure measurement device,

- Any particularity of the conducted experiment influencing the final configuration of the model, has to be considered prior to its development. It is usually more difficult to modify an existing model to meet the needs linked to new experimental configurations than foreseeing these needs and creating the model accordingly. For the current experiment, openings on the side walls of the cube had to be created in order to test the natural cross-ventilation of the cubical model. Furthermore, the pressure tubing was passed through an internal central column of rectangular cross section, to facilitate geometry reconstruction in the future.

- Additional elements which may be required for experimental configurations other than the basic one, should also be developed according to the needs arising from a specific application. For the current experiments, three porous materials (one with PPI60 and two with PPI20 i.e. 20 pores per inch) were chosen and cut to the correct size, in order to be installed as façade and roof greenings (simulated vegetation).

- Finally, mounting of the model on the surface of the wind tunnel should also be considered. In the present case, pressure tubing exited the model through a brass tube fixed to the model's floor. This tube was used to mount the model onto the wind tunnel floor.

The top view and the side view of the cubical model can be seen in Figure 12 a and b respectively. In Figure 12a one can observe the pressure taps installed on the roof whereas in Figure 12b the side opening is visible.

a)   b)
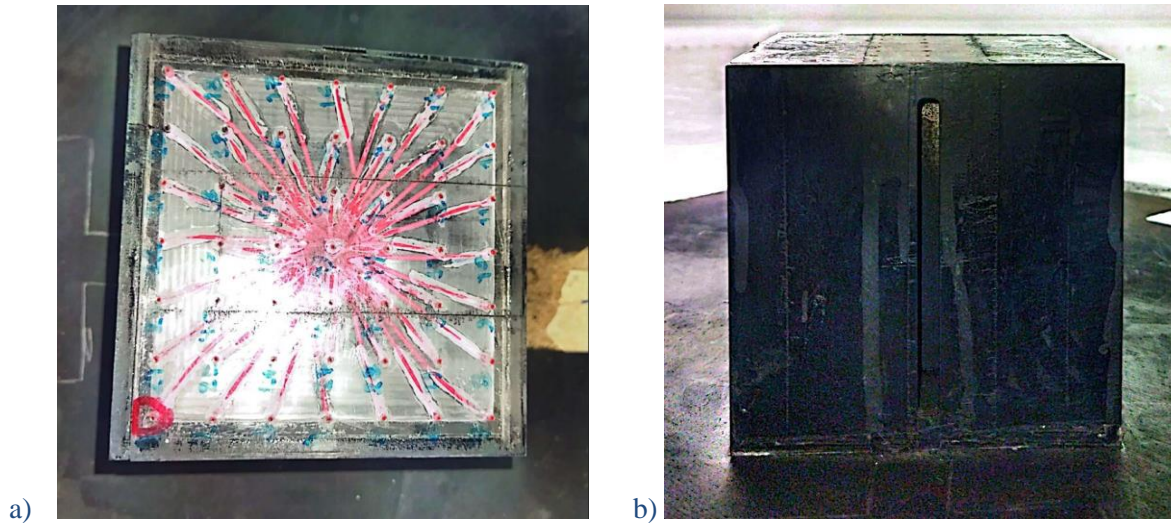
Figure 12 *Model of the cube: (a) top view and (b) side view*

3.2.2 Measurement Planning

Careful design of the experiments, planning and time management can play an important role in the success of any experimental campaign. A few general steps are proposed as follows:

- conceptual design of the experiment after having thoroughly reviewed the available literature on the specific subject in order to: (a) find literature "gaps" and (b) acquire the necessary knowledge for the completion of the experiment. If there are already available results pertaining to the chosen research subject, then this should be considered as early as possible, in order to enable future comparisons. In the case of the current experiment, LDV measurement results were already available from experiments conducted at Karlsruhe Institute of Technology (KIT) and the PIV measurement planes were chosen to coincide with the coordinates of these measurements.
- Development of a detailed Gantt chart containing all the necessary individual tasks, their starting and ending times as well as a brief description corresponding to each of them. In particular, for the determination of the duration of each task, quantifiable measures/indices have to be used when possible. For the case of PIV measurements, one can calculate the required measurement time by considering the pulse separation time of the laser, the time between every snapshot, the desired number of snapshots etc. In a more practical approach, some sample measurements can be taken and used as a measure to extrapolate the required measurement time.
- Listing of potential problems linked to the proposed research and attempting to find possible solutions. This may lead to reconsideration of the initial measurement planning. However, it should be kept in mind that setbacks will always occur and measurement planning should account for unforeseen events.
- Ensuring availability of facilities and equipment for the duration of the measurements is of paramount importance in order to avoid potential conflicts with the planning of other researchers who may be using the same equipment.

All the aforementioned actions should be undertaken and organised in agreement with all participating members (supervisors, colleagues etc). Discussion with more experienced researchers prior to or during the measurement planning and time management, is always recommended.

3.3 Quality Assurance

3.3.1 PIV measurements

3.3.1.1 Camera positioning and calibration

For positioning the camera for Mono-PIV, the view of the camera should be normal to the plane of measurement (e.g. see Figure 13) and that the entire measurement plane is viewed by the camera. It is imperative that all points of the measurement plane, defined by the laser light sheet, should be in focus. In this sense, it is recommended to use the calibration target (see Figure 14), position it in-plane with the light sheet and define the correct zoom settings of the camera, so that all white markers of the calibration target are clearly visible.
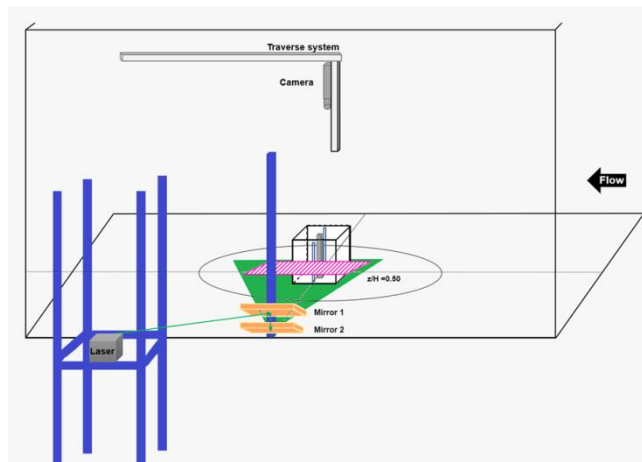
Figure 13: Mono PIV configuration set-up of side wall horizontal measurement planes, at two heights: $z = 0.5H$ and $z = 0.75H$, where H is the height of the cube. In the framework of the current experiment, measurements were undertaken for the horizontal plane with $z = 0.75H$
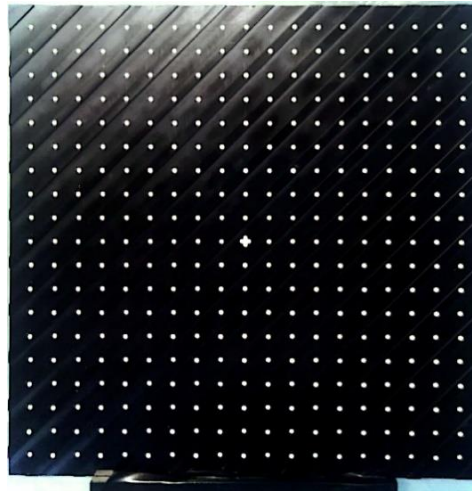
Figure 14*: PIV calibration target.*

a)

b)

c)
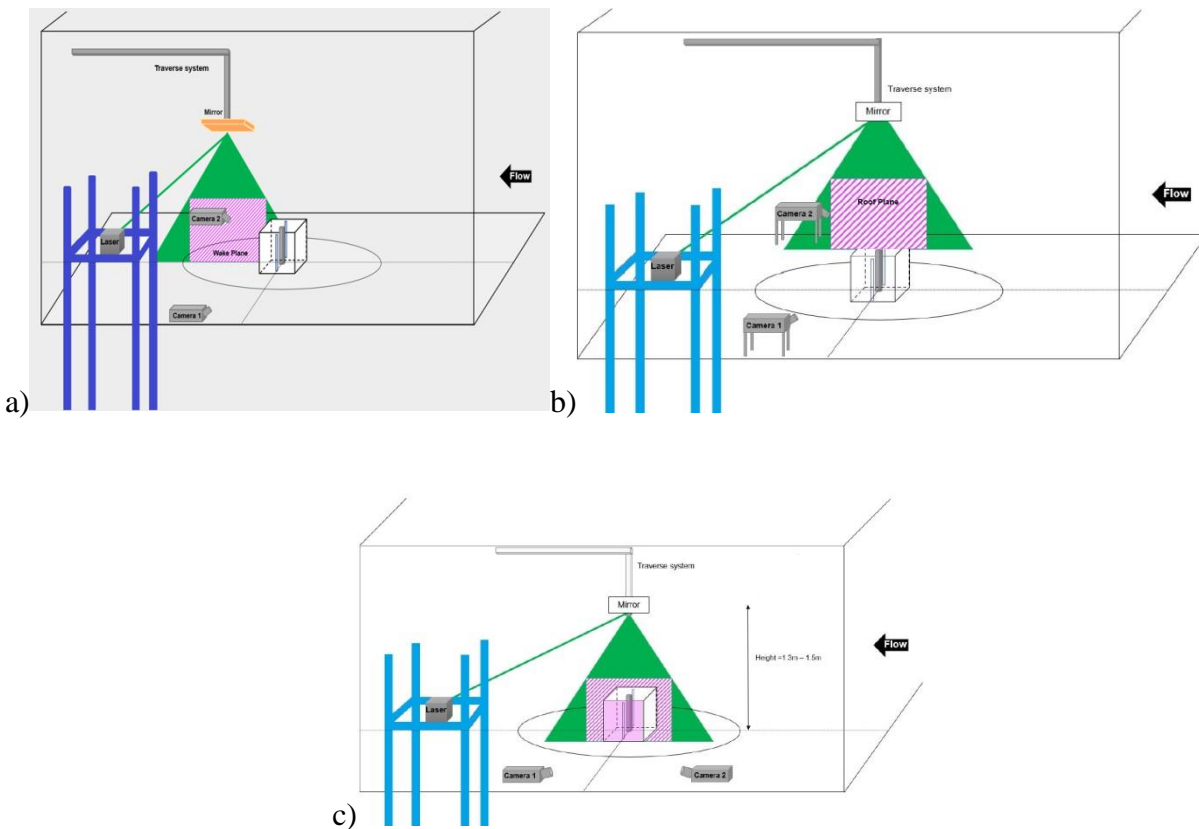
Figure 15 *Stereo-PIV configurations for three different measurement planes (a)* Wake plane*, (b)Roof plane and (c) Lateral Plane (parallel to the flow)*

For the Stereo-PIV configuration, the requirements for camera positioning and calibration are significantly more complicated than the respective ones for the Mono-PIV. However, it is once again recommended to initially use the calibration target to define the correct zoom settings for both

the cameras so that all white markers of the calibration target are clearly visible by each camera, similarly to what was done for the Mono-PIV configuration. It is also recommended that the fiducial marker of the calibration target is located at the center of both calibration images captured by the two utilised cameras or at least at a point which has the same coordinates for both images. Although there are several configurations to acquire the desired measurements i.e. planar measurements of all 3 velocity components (2D-3C), usually the main requirement is to place the cameras so that the Scheimpflüg condition is respected for each of them. This means that the object plane (light-sheet), image plane, and lens principal plane should intersect at a common point and, this is accomplished by appropriately and gradually tilting the camera body with respect to its lens so that this condition is satisfied. By trial-and-error procedures, one can ensure that the Scheimpflüg condition is respected and the image will be in focus throughout the measurement plane. The fulfillment of the Scheimpflüg condition (and generally the oblique view of the measurement plane) deliberately leads to a perspective distortion i.e. the magnification factor (ratio of an image length scale to the respective, real one) is not constant across the examined plane. This leads to a necessity of a more complex calibration procedure with which it is sought to define the aforementioned magnification factor for the whole examined plane. Although it is common to place the two cameras symmetrically with respect to the plane of measurements, a more general configuration [11] is where the only requirement is to ensure that the viewing axes of the cameras are not collinear. The angle between the cameras should be 60-90° with the optimal angle being 90° [11]. The applied configurations for the current Stereo-PIV experiments are shown in Figure 15. For the current application, TSI PowerViewPlus 4MP cameras with a CCD array of sensors employing frame straddling [11] are used whenever PIV images are acquired for the actual flow field measurements.

3.3.1.2   *Laser positioning, alignment and operation*

The laser apparatus comprises two individual laser beams (laser 1 and laser 2) in order to ensure the very fast laser pulse necessary for PIV applications, which a single laser beam could not provide at a reasonable cost. The laser used in the present application is a Lytron Nd:YAG with a nominal energy of 200 mJ per pulse, which is frequently used in PIV applications since it has a high amplification and good mechanical and thermal properties [11]. Within the apparatus are the two lasers, which should produce laser sheets that are in perfect alignment with each other, both horizontally and vertically. Misalignment will result in non uniformly lit images and low quality or unusable data. The beams should also exhibit similar intensity properties (same shape of laser beam, same intensity across the field of illumination of the lasers etc.). In general, this alignment is effectuated by appropriately tuning the available optical systems involved in the generation of the laser sheets (reflectors, optic lenses etc.). Each laser manufacturer has equipment specific instructions for laser alignment.

For generating the correct measurement plane within the flow domain, the laser sheet must be directed and aligned properly. Figure 16 shows an example of this procedure, using the calibration target. The green laser sheet is initially generated in the horizontal direction and turned vertically via the mirror suspended above the target plane. As long as the full plane of the target is uniformly illuminated by the laser sheet (low laser intensity can be used for this test), the camera focus on the target can be assumed to also focus on the illuminated plane (after the target is removed for measurements). The red laser line illuminating the side of the calibration target ensures the vertical positioning of the target.

The alignment procedures can and should be performed with the laser at low intensity. General operation of the laser should be performed in accordance to the instructions enclosed in the respective manuals.
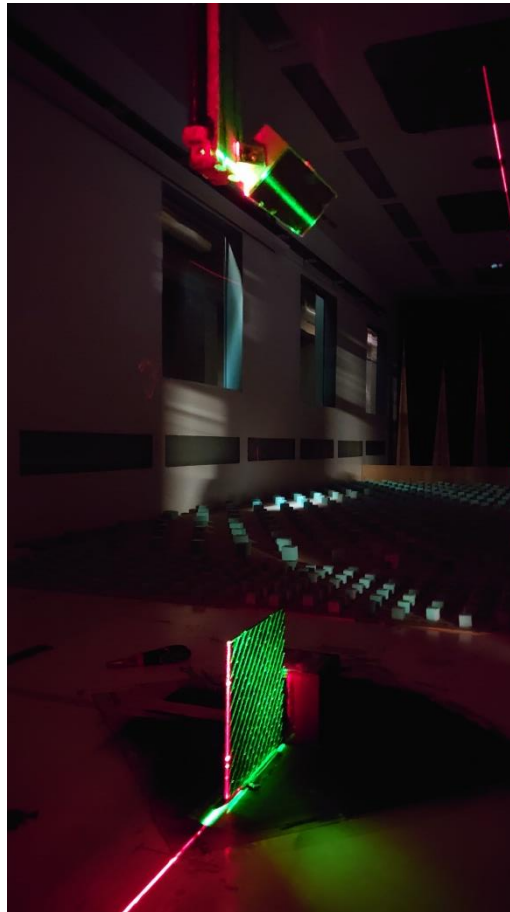
Figure 16 Using the calibration target to align the laser sheet.

3.3.1.3 Seeding Quality

In PIV measurements, it is actually the velocity of the seeding particles that is measured rather than that of the flow. If proper attention is not paid to the seeding quality, then significant discrepancies between the motion of the particles and that of the flow can arise and affect the conclusions of the flow study. More specifically, as denoted by [11] there are two contradictive requirements regarding the size of the particles:

- The size of the particles has to be very small in order for them to follow the flow. This requirement is represented by the Stokes number of the seeding particles within the fluid medium [11].
- The number and size of particles has to be sufficiently large in order for the light scattering to be efficient. Although the light scattering is a process that depends to multiple parameters (e.g. ratio of the refractive index of the particles to that of the surrounding medium, particles' size, their shape and orientation etc.), it is generally observed that the scattered light intensity increases with increasing particle diameter [11].

Another aspect of the light scattering that has to be considered is the fact that the light is not scattered uniformly in all directions. Usually, there are local maxima and minima of the scattered light intensity with respect to the direction of the scattering.

Although in heavily seeded flows multi-scattering due to more than one particle can increase the image intensity and possibly the contrast of the captured images (key component in order for the velocity vectors to be extracted) it can also introduce background noise and thus higher levels of noise in the recorded images. On the other hand, increased number of seeding particles enhances the signal strength of the correlation peak and also yields a better spatial resolution, capable of revealing smaller flow structures.

All the aforementioned points lead to the conclusion that two compromises are generally made for the seeding of air flows: (a) the size of the particles should take such a value so that they adequately follow the fluid flow while at the same time possess the desired light scattering properties; (b) the number of seeding particles has to be sufficiently high to ensure proper and relatively uniform illumination of the examined domain without introducing too much background noise. A rule of thumb ([9] , [12]) is that particle image pairs per interrogation spot have to be more than ten to ensure a high percentage of correct velocity measurements.

When air flows are examined, health considerations are of great importance since the experimentalists may inhale seeded air e.g. in wind tunnels with an open test section [11]. Furthermore, the infiltration of the particles into the test section has to be carried out without disturbing the flow and in a way that ensures homogeneous distribution of the tracers. To accomplish the latter, it is recommended to start the injection of the seeding particles prior to the acquisition of images (in the current case this was done for about 5-10 minutes between every individual experiment). Preferably, some images depicting the seeding of the flow should be captured before obtaining actual measurements, in order to suitably adjust the inflow of the particles. When the correct setting for the seeding is found, minimal or no changes at all have to be made in all the participating components (system of pressurised air, droplet generator etc.) throughout the whole experimental campaign, so that a reference seeding situation is maintained.

Regarding the type of seeding particles for air flows, [11] give specific instructions while they denote that for their applications, they use oil or DEHS particles. In the current application olive oil was used as the seeding material while a commercial droplet generator (TSI model 9307) producing droplets of diameter 1-2 μm (see [13] [14]) was employed.

3.3.1.4   Background noise elimination

Although there are numerous sources of noise/errors such as electrical noise from the utilised cameras, inappropriate seeding particle diameter and density of the seeding, numerical noise/errors due to the employed PIV evaluation method etc. here the main focus is on the elimination of the background noise due to artificial/natural lighting during the PIV experiments. For a full quantification/examination of PIV measurement uncertainty, the reader is referred to [11].

As already mentioned, in order for the PIV evaluation to be properly effectuated, there has to be a contrast between the illuminated seeding particles and their background. In case where artificial/natural lighting intrudes into the testing section, measures have to be taken to ensure that the final results won't be contaminated with background noise. Hence, windows or other openings permitting the intrusion of light have to be appropriately covered. Moreover, light scattering due to reflective surfaces/objects exposed to the laser-sheet, near the experimental domain, has to be prevented. On many occasions, painting the floor black in close vicinity of the model is a good measure to ensure the desired contrast between the illuminated particles and their background,

especially when conducting measurements on a plane parallel to the floor. A general rule of thumb is to keep the background of measurements as uniform and dark as possible.

3.3.1.5 Exposure and pulse separation time

Generally, there are a number of options available regarding the way that the seeding particles are being exposed to the illumination source and subsequently recorded by the camera(s). This mainly depends on the type of laser and recording camera(s) that are utilised as well as on the capabilities of synchronisation of all these components through appropriate hardware and software. There are two general approaches regarding this matter [11]: (a) single-frame/multi-exposure and (b) multi-frame/single-exposure. The first category is based on the following principle: seeding particles are exposed to multiple pulses (or to a continuous one for certain time instants), and the results of these multiple exposures are stored in a single frame. Thus, the only choice in order to retrieve information for the displacements of these particles is to perform autocorrelation between this frame and itself. The main disadvantage of this approach is that it cannot identify the direction of the displacement of a particle image (directional ambiguity) unless special care is taken, since the exposures corresponding to specific time instants are all stored together.

When multi-frame/single-exposure approaches are implemented, this ambiguity ceases to exist, since every exposure corresponds to a specific frame. In the present case, double frame/single-exposure measurements are conducted. In this case, the PIV evaluation is accomplished by means of cross-correlation between the two captured frames. The duration of the pulse illumination (exposure) should be sufficiently short [11] so that the motion of the particles can be instantly captured without any image blurring and "streaks". However, it is difficult to make a general recommendation regarding exposure since it is influenced by a variety of factors such as laser energy, light sheet dimensions, camera focal length number, photograph magnification, film speed and resolution, particle size, and particle material [9]. In particular, the complex nature of particle light scattering (it is in the Mie regime for most PIV applications) is the main reason that prevents the extraction of a general guideline regarding the duration and the intensity of the exposure for PIV applications [9].

The optimal pulse separation time is strongly related to the physics of each examined PIV application. A general guideline is that the pulse separation time (time delay between two subsequent pulses) has to be long enough in order to yield a discernible displacement peak in the correlation plane (regardless of the way that the exposure, the recording of images and the respective PIV evaluation are effectuated) [11]. However, it should also be short enough in order to reduce the number of fleeting particles due to out-of-plane motion [11]. Small pulse separation times are preferable [14] when the reduction of errors linked to flow acceleration and curvature effects is desired while it is also clarified that as the pulse separation time decreases, the measurement dynamic range (i.e. range of reliably measured velocities) also decreases. So, clearly there is a contradiction, and a compromise has to be made. An equation relating the pulse separation time with the percentage of particles present in both frames of a PIV recording for a plane normal to the flow is given by [15].

3.3.1.6 Stability of the PIV cameras

When the wind tunnel operates, issues related to unwanted camera vibration may occur, particularly if the cameras are not securely mounted to the floor of the wind tunnel (e.g. when measuring velocities on a horizontal plane, see Figure 13). The following procedure was followed in order to quantify the degree of unwanted movement of the camera:

- Perform image intensity measurements without operating the wind tunnel. A reference mark which has distinguishably different image intensity from its background is used. The boundary of this mark can be used as a detector of incident movement of the camera. In the current case, a (+) sign was created on the wind tunnel floor, using black duct tape on the white tunnel floor.

- The same measurements are undertaken for the case of maximum free stream velocity to be applied during the experiments. It is suggested to perform the same measurements in both the empty wind tunnel and the wind tunnel with a specific atmospheric boundary layer (ABL) desired to be simulated, using roughness elements and spires. In the former case, maximum velocities are expected across the entire cross-section of the tunnel, while in the latter case, maximum turbulence intensity is ensured.

- Finally, possible vibration or other displacement of the camera can be detected by carefully examining image intensity profiles, containing part of or the entire boundary (or boundaries) of the reference mark.

- This procedure is repeated for every participating PIV camera.

3.3.2   Wind Tunnel background flow

A variety of preliminary measurements/tests may be required in order to establish that the wind tunnel background flow demonstrates the desired properties for a particular test. In the cases of the current book of reference, three types of complementary/preliminary measurements were effectuated: (a) hot-wire measurements for the Atmospheric Boundary Layer (ABL) characterization as well as the extraction of the reference velocity, necessary for the calculation of Reynolds (Re) number; (b) pressure measurements for the verification of flow symmetry inside the test section. A brief explanation for every set of preliminary/complementary measurements is read as follows:

3.3.2.1   ABL characterisation and reference velocity:

Hot-wire velocimetry/anemometry is employed for the acquisition of high-frequency velocity measurements. For the experiment presented here, a hot-film Model 1201 TSI probe [16] was employed for ABL characterisation and measurement of the reference velocity at the height of the cube. For the former, a comparison with previous ABL measurements (in the same test section) and well-established standards (e.g. VDI [17], Eurocode 1 [18]) is required, in order to verify that indeed the developed ABL profile possesses the desired properties for the current application, i.e. corresponds to the profile that is typically encountered in real flows for a specific terrain (e.g. suburban, urban etc.). For more details regarding the procedure of ABL characterisation the reader is referred to [8] and [13]. The measurement of the reference velocity is effectuated at the height of the cube, in order to establish that the minimum requirement for Re-independence [19] is respected throughout the experiment. Obviously, this is necessary due to the fact that it is almost always impossible to ensure that the same Reynolds number with that of the full scale is obtained during reduced-scale wind tunnel experiments. It is strongly recommended to calibrate the hot-film (using a Pitot tube) as frequently as possible, ideally one or two times per day. The calibration procedure of the hot-film is out of the scope of the present book of reference.

3.3.2.2 Flow Symmetry

After having placed the model of the cube at the center of the turn-table of the test section, flow symmetry should be verified by appropriate measurements. Although there is the option to conduct hot-wire velocity measurements at symmetric points with respect to the cube's centerline and at height equal to the cube's height, here a different approach consisting of pressure measurements was adopted due to its relative ease of application (e.g. no calibration is required). The building model has pressure taps installed on its roof, which are easily connected to a pressure sensor via appropriate tubing system. The top view of the cube containing the specific pressure taps that were used for investigation of flow symmetry is shown in Figure 17. Hence, a value of zero for the pressure difference between the two pressure taps indicates that flow symmetry is probably established for the flow past the cube.
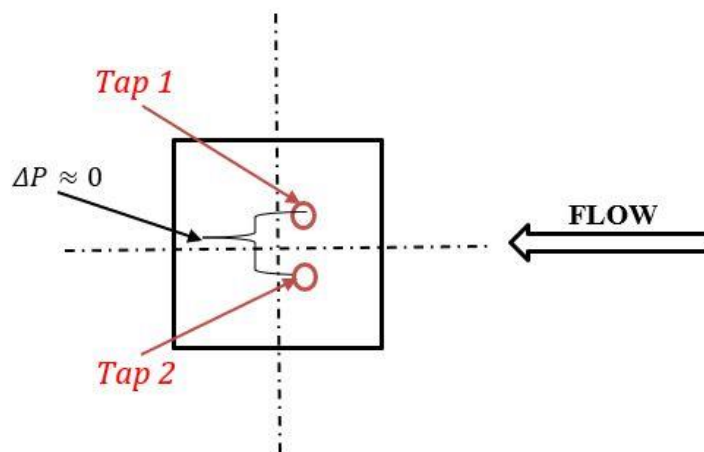

Figure 17*: Top view of the cube, including the pressure taps used for the establishment of flow symmetry.*

3.3.3 Preliminary Data Processing

The processing procedure for the extraction of the velocity vectors from the PIV snapshots, captured by the high-speed camera(s) consists of four main steps which are independent of the utilised processing software.

3.3.3.1 Calibration of the camera(s)

A calibration using a calibration target has to be done prior to the undertaking of the experiments in order to ensure that the image is sufficiently clear and focused (all white markers in Figure 14 are distinguishable from their background i.e. the black area of the calibration target) and also to acquire necessary functions which will map the results from the image space to the real space (conversion from pixels to meters). For Mono-PIV, where a constant magnification factor is present, the calculation of this magnification factor can be performed using the known distance (meters) between two white markers of the calibration target. Alternatively, every object with known dimensions in the real space (meters) and in the image space (pixels) can be used as a calibration source.

The procedure is significantly more complex for Stereo-PIV since the magnification factor is not constant (perspective distortion). For this reason, four calibration images (for both frames and

for two cameras), containing the calibration target at a location which coincides with the measurement plane, have to be acquired. Then the mapping functions responsible for the conversion from pixels to meters and equivalently from pixel/s to m/s can be calculated and applied to the extracted raw data, after the end of the experiment. This conversion becomes feasible by identifying all white points marked on the calibration target, whose coordinates are (or have become) known in pixels and in meters (or at least the distance of a pair of markers since they are all equidistant).

However, the aforementioned mapping does not encompass any information for the viewing angles of the cameras so that the three-component velocity vector can be reconstructed. To obtain this information, a set of image-to-object correspondence points that are not coplanar is required [11]. That's the reason why the target has calibration marker points that alternate between two depths (most visible in the top left corner of Figure 14). This type of calibration target is called a four-plane target (2 planes of marker points on each side).

Finally, a masking step is also included in this procedure. The image is masked/cropped to the area where measurements are desired. This allows for exclusion of parts of the image that are outside the calibration markers or susceptible to noise, reflections etc.. In the case of Stereo-PIV, the same procedure has to be effectuated for two images, corresponding to the two employed high-speed PIV cameras. Note that there are also other types of calibration targets [9] as well as ways to obtain information for the viewing angles [11].

3.3.3.2 Pre-processing of raw data/images

This step aims to eliminate noise, principally caused by artificial or natural lighting during the experiment, and has to be taken care of before the capturing of PIV snapshots. The point of minimum intensity, almost always corresponding to a point in the background, is found from a group of PIV snapshots and then subtracted from every image/snapshot in the group to be processed. Care should be taken to avoid including outlier images in this procedure e.g. unsynchronized black images. It is clarified that for every employed camera two minimum intensity frames are usually produced, i.e. frame A and frame B. Then these minimum intensity frames, are subtracted from every frame of each snapshot, respectively, to eliminate the background noise. In that way, the position of the seeding particles which are captured by the camera(s), can be reliably identified since their contrast with respect to the background is enhanced. Overall, this is a procedure to enhance image intensity values and may appear in a number of variations, depending on the user's experience.

3.3.3.3 Processing (calculation of velocity vectors)

Generally, this step of the processing procedure is the most computationally-intensive. Therefore it is usually not applied straight away but initially using a subset of the whole group of snapshots before applying it to the whole set. This allows for trial and error definition of the correct setup of parameters. In this step, the employed PIV evaluation algorithm e.g. (digital) cross-correlation-based, is applied for the extraction of the velocity vectors. Note that prior to the advancement of computers, PIV evaluation was usually effectuated using purely optical methods instead of digital, finding or approximating the autocorrelation instead of the cross-correlation function [11]. Every software provides a rather large number of possible combinations of parameters to effectuate this kind of processing procedure. These parameters are usually determined by consulting the manual of the employed software in conjunction with trial-and-error tactics. When these parameters are fixed, then one can proceed to the processing of all extracted PIV snapshots. Although it is possible that determination of different parameters may be required for

different software, a general description of them will be illustrated, using as starting point the available choices given in TSI's INSIGHT 4G software. The parameters that have to be generally determined are:

- the shape of the PIV grid cells (interrogation windows). For example uniform or non-uniform grid, cartesian or non-cartesian (e.g. with rectangular, square or custom-made interrogation windows). Generally, the most common choice is to use cartesian and uniform PIV grids (e.g. NyquistGrid option of Grid Engine in INSIGHT 3G or 4G).
- the size of the interrogation window. This interrogation window determines the number of sub-regions/cells utilized to calculate the cross-correlation plane of image intensities. From this calculation, the displacement peak within a specific interrogation window can be extracted and by knowing the time between the two captured frames, the interrogation-window-averaged velocity can be acquired. The purpose is to extract the displacement of seeding particles. Usual choices for the size of the interrogation window are 32×32 $pixels^2$ and 64×64 $pixels^2$. Under certain circumstances, the PIV algorithm may "pass" from an initial larger interrogation window to a smaller one in a recursive manner making use of calculated displacements corresponding to the previous larger interrogation areas. Then, these displacements are used to shift the interrogation areas from their initial position in order to increase the signal-to-noise ratio (i.e. higher number of matched particle pairs, [11]). In that way, the final velocity vectors are characterized by a higher spatial resolution as well as increased signal-to-noise ratio (there are less fleeting particles due to in-plane motion). Another possibility is to use deformed and smaller interrogation windows in subsequent "passes" according to the calculated displacements of the previous passes in order to optimise the PIV evaluation procedure (i.e. the assumption of uniform displacements within an interrogation window is discarded, [11]). Note that, although a smaller size of interrogation windows could potentially yield more information, it could also lead to higher processing times as well as to difficulty of properly calculating/identifying velocity vectors. As [11] denote, below a certain number of matched (particle) pairs in the interrogation area (typically less than 4), the detection rate and thus the capability of the method in velocity calculation will decrease rapidly. A higher value of the underlying signal-to-noise ratio permits the utilisation of smaller interrogation windows improving the final spatial resolution of the extracted velocity field. This signal-to-noise ratio depends on various parameters such as the quality of the illumination as well that of the seeding, the capabilities of the employed cameras and the respective cable connections, out-of-plane motion of particles for 2D measurements etc. [11]. Finally, for the sake of completeness, it is denoted that Particle Tracking evaluation methods based on the calculation of the displacement of individual particles instead of the average values of entire interrogation windows, is also a possibility for specific applications where the necessary computational sources are available.
- the mathematical/numerical method that has to be employed for calculation of the cross-correlation in order to be able to identify the displacements of seeding particles, as already explained. One typical option is to employ FFT to undertake this calculation (default option in INSIGHT 4G). Finding the cross-correlation function through FFT significantly saves computational resources instead of directly calculating it [11].
- the peak intensity to noise ratio. This is basically the ratio of the (global) maximum of the 3-D cross-correlation function (between the examined interrogation window and all the others) to the second highest (local) maximum which probably corresponds to noise,

Co-funded by the European Union

3. NTUA - Equipment and methods. Applied Knowledge.   35

unavoidably existing in every measurement. Typical values of this ratio range from 1.3 to 1.5.

Although there are additional parameters for the processing of the images, it is important to note that there is not one universally applicable combination of parameters in order to acquire satisfying velocity measurements. This means that the correct setup for the extraction of velocity vectors, for a particular experimental configuration can only be found through trial-and-error tactics. Note that this procedure could be quite time-consuming, and this has to be kept in mind when a new experiment is designed. However, an index that can intuitively lead to the correct set-up of parameters is the ratio of "good"-to-"bad" vectors. A high value of this ratio usually indicates that the processing of the images is successful. Finally, it is strongly advised for experimentalists who have no previous experience in PIV measurements to pay attention to the theoretical/mathematical background of PIV evaluation methods (e.g. how the cross-correlation is applied, why FFT is used and in what way etc.) prior to their first PIV experiment. In that way, every choice of parameters and evaluation methods will not be made blindly but through careful examination of the underlying physics of the specific problem, knowing the limitations of the aforementioned choices.

3.3.3.4 *Post-processing (calculation of velocity vectors)*

The previous step of the processing procedure, i.e. the extraction of velocity vectors from the PIV snapshots may result in certain "bad vectors". This means that by applying user-defined criteria, an amount of the extracted vectors may be classified erroneous. After discarding the erroneous vectors, the vector field may contain "gaps" instead of the (erroneous) vectors and therefore, they have to be filled with velocity information. Besides, it is possible that "gaps" within the initial velocity vectorial field are already present due to issues such as poor illumination of specific regions of the plane, optical access problems, insufficient seeding etc. So, this step has a twofold aim: (a) identification of the erroneous vectors and (b) compensation in terms of velocity information due to loss of velocity vectors caused by issues linked to the experimental procedure and/or non-satisfaction of user-defined validation criteria.

The user-defined validation criteria of the velocity vectors are usually either local or global. An example of a local criterion is one specifying that if the velocity magnitude value of a particular PIV velocity vector significantly differs, beyond a certain threshold, from the average value of its neighbouring PIV vectors, then this velocity vector is labeled as a spurious one. On the other hand, a global criterion example could be similar to the latter local one, with the difference being that the global average of the velocity magnitude of the whole vectorial field is used instead of the local average, described above. For the case of Stereo-PIV, it is possible that the 3-D processing for the acquisition of the third velocity component happens after this step. For more detailed presentation of existing validation/post-processing methods the reader is referred to [11] and [20].

For the already mentioned compensation of velocity information, one illustrative solution is filling the "gaps", existing within the plane of measurements, by using the average value of certain (their number is user-defined), neighbouring PIV velocity vectors. Common algorithms to effectuate this post-processing step start from "gaps" where values of adjacent PIV cells are available and continue recursively to compensate for all lost velocity information.

4 Twin Test #1: Effects of Vegetation on Flows in the Urban Environment

4.1 Boundary Layer Characterisation

4.1.1 KIT

A view of the test section upstream of the turntable in the boundary layer wind tunnel at Karlsruhe Institute of Technology (KIT) is shown in Figure 18. Geometrical parameters of the test section are as follows:

- Tunnel cross section (width × height): 2.0 m × 1.0 m, confined by smooth vertical walls and ceiling.
- Adjusted ceiling for zero pressure gradient in the streamwise direction (dp/dx = 0).
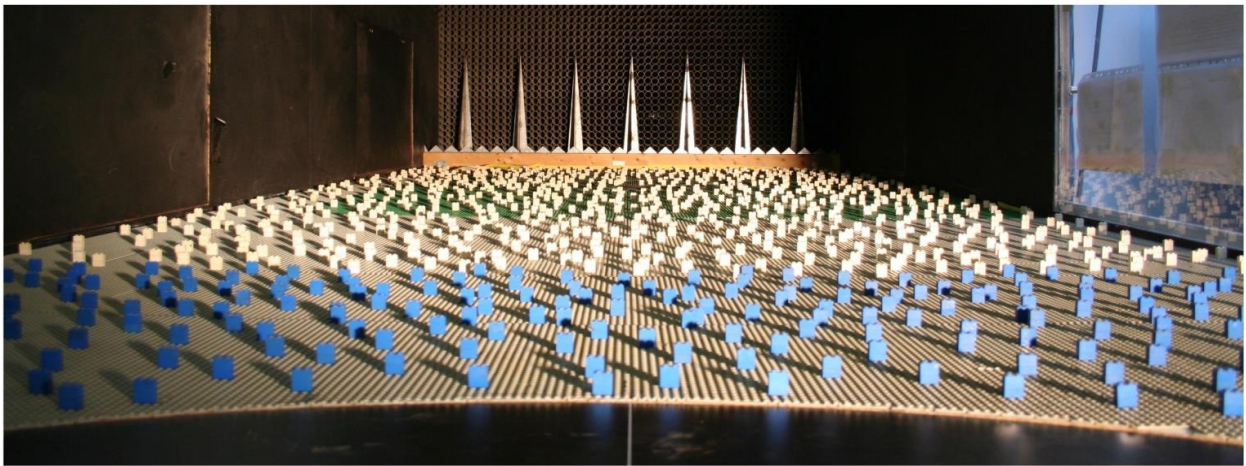
Figure 18. Set up of the fetch of the atmospheric boundary layer (ABL) upstream of the turntable at KIT.

For the measurement of the boundary layer profiles of mean velocity and turbulence intensity, a constant temperature hot wire anemometer was used with a single wire probe, aligned with the flow, and a sampling frequency of 6 kHz for an acquisition time of 60 s.

The flow parameters that were extracted from the measurements are presented in Table 1, where H is the height of the building model. Both the calculated power law exponent $\alpha = 0.28$ ($0.24 \leq \alpha \leq 0.40$) and the full-scale aerodynamic roughness length $z_o = 0.54$ m ($0.50 \leq z_o \leq 2.0$) correspond to the lower limits of an urban atmospheric boundary layer, i.e., the flow over inner city center and are just above those of a suburban setting.

Table 1 Flow parameters for twin test at KIT

Power Law	$$\frac{u(z)}{u_{ref}} = \left(\frac{z-d}{z_{ref}}\right)^{\alpha}$$	z_{ref} = H =110 mm U_{ref} = 3.27 m/s d = 0 α = 0.28
Logarithmic Law	$$\frac{u(z)}{u_*} = \frac{1}{\kappa}\left(\ln\frac{z-d}{z_0}\right)$$ *(applicable up to 0.15δ height)*	u_* = 0.25 m/s z_0 = 1.80 mm κ = 0.4 d = 0
Reynolds number, Re_H based on building height and U_{ref}		2.35 ×10^4
Free stream velocity, u_∞		5.0 m/s
Scale factor, M based on VDI guidelines		1:300

4.1.2 NTUA

A view of the test section upstream of the turntable in the boundary layer wind tunnel at the National Technical University of Athens (NTUA) is shown in Figure 19. Geometrical parameters of the test section are as follows:

- Tunnel cross section (width × height): 3.5 m × 2.5 m, confined by smooth vertical walls and ceiling.
- Adjusted ceiling for zero pressure gradient in the streamwise direction (dp/dx = 0).

Figure 19 Set up of the fetch of the atmospheric boundary layer (ABL) upstream of the turntable at NTUA

4. Twin Test #1: Effects of Vegetation on Flows in the Urban Environment
4.1 Boundary Layer Characterisation

For the measurement of the boundary layer profiles of mean velocity and turbulence intensity, a constant temperature hot wire anemometer was used with a single film probe, aligned with the flow, and a sampling frequency of 10 kHz for an acquisition time of 104 s.

The flow parameters that were extracted from the measurements are presented in Table 2Table 1, where H is the height of the building model. It should be noted that a building model of same geometry was used at KIT and NTUA. Both the calculated power law exponent α = 0.22 (0.18 ≤ α ≤ 0.24) and the full-scale aerodynamic roughness length z_o=0.39 m (0.1 ≤ z_0 ≤ 0.50) correspond to the suburban atmospheric boundary layer, i.e., the flow over park/suburban area.

Table 2 Flow parameters for twin test at KIT

Power Law	$$\frac{u(z)}{u_{ref}} = \left(\frac{z - d}{z_{ref}} \right)^{\alpha}$$	z_{ref} = H = 110 mm U_{ref} = 2.36 m/s d = 0 α = 0.22
Logarithmic Law	$$\frac{u(z)}{u_*} = \frac{1}{\kappa} \left(\ln \frac{z - d}{z_0} \right)$$ #applicable up to 0.15δ height	u_* = 0.22 m/s z_0 = 1.45 mm κ = 0.4 d = 0
Reynolds number, Re_H based on building height and U_{ref}		1.65×10^4
Free stream velocity, u_∞		5.0 m/s
Scale factor, M based on VDI guidelines		1:270

4.1.3 KIT-NTUA Wind tunnel ABL flow comparison

Comparison of the velocity measurements performed at the wind tunnel in KIT and NTUA to characterize the simulated atmospheric boundary layers are presented in Figure 20 and turbulence intensity and calculated turbulence integral length scale in Figure 21. Although the profiles correspond to an urban (KIT) and suburban (NTUA) ABL category, they are at the lower and upper limits of these and, as their comparison reveals, they are similar and comparable up to roughly two building heights. This holds both for the mean velocity and the turbulence intensity. The turbulence integral length scales are also comparable up to one building height from the ground, with the NTUA values increasing above this height, most probably due to the higher test section in the NTUA wind tunnel.

The results are considered favorable for comparing measurements in the two wind tunnels and, given that the building Reynolds numbers in both the KIT and the NTUA wind tunnels are above the 10^4 threshold for Reynolds number independence, it is expected that the measurements of the flow past the same building model will provide valuable insight through cross-comparison.
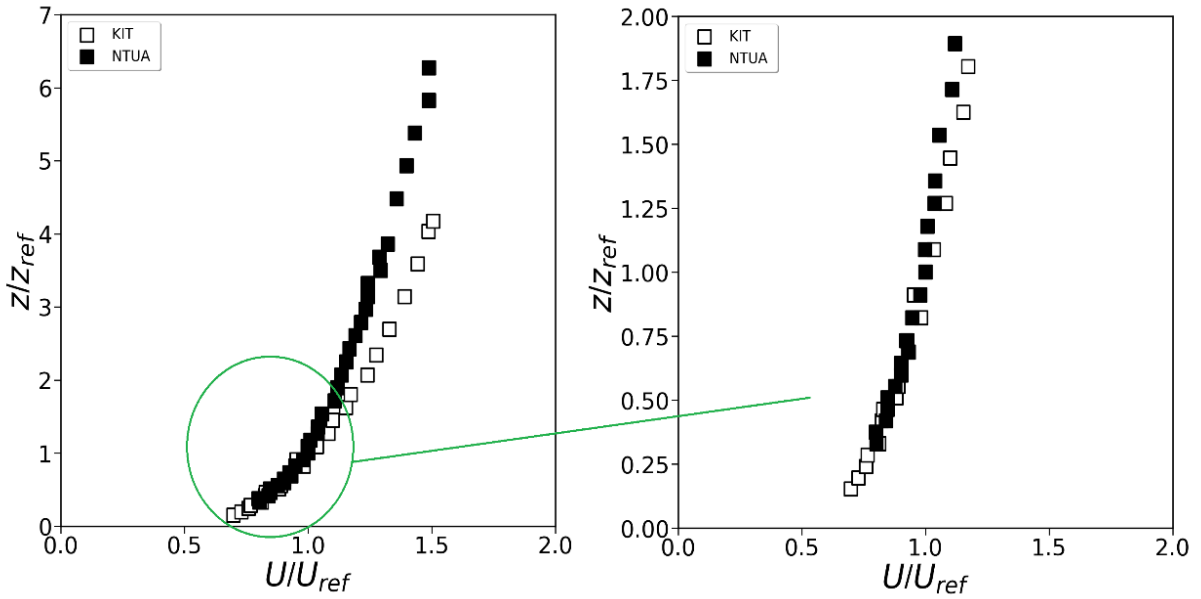
Figure 20. Measurements of the velocity profiles at the center of the turntable, without building model for the full vertical span of the measurements (Left) and for two building heights above the floor level (Right)
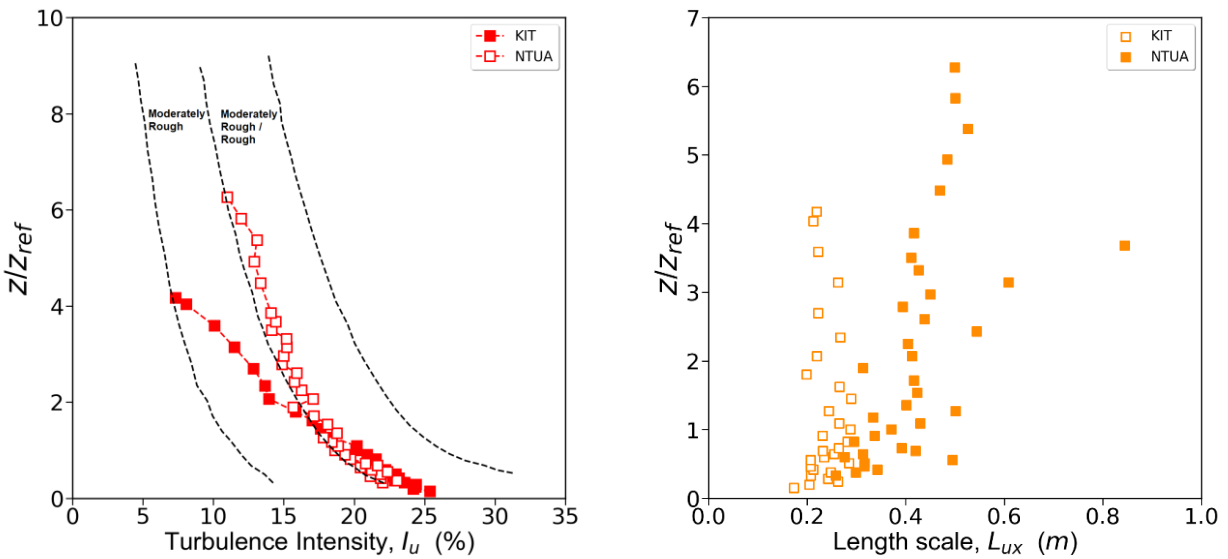

Figure 21. Measurements of the turbulence intensity (Iu) profile (Left) and calculated ~~turbulence~~ integral length scale (Lux) (Right), at the center of the turntable, without building model.

4.2 Experimental Configurations and Settings

The twin test involved measurements of the flow past a surface mounted cube, exposed to an atmospheric boundary layer. The cube is intended to represent a building at a scale of 1:300, in agreement with the ABL scales extracted from the measurements in Table 1 and Table 2. The height of the building model was H = 110 mm, and the vertical openings on its side were: (height), h_e = 90 mm and (width), w_e = 6 mm. Inside the building, in the center, there was a vertical column of square cross section (22x22 mm^2).

Besides the basic flow past the building model with smooth outer walls, tests were performed with modelled vegetation covering the windward façade and the roof of the building. Vegetation was modelled with open-cell reticulated foam materials and results are presented here for foams with a pore density of 60 PPI of 10 mm thickness, corresponding to a full scale (1:300) permeability value of λ_{fs} =7.82 m^{-1}, which corresponds to dense hedges. Details on the permeability measurements and the scaling procedures for the foams can be found in [8].The test configurations are shown in Figure 22 and are common for the tests in the KIT and the NTUA wind tunnels.

It should be noted that tests were also performed, over and above those initially planned during the TWEET-IE twin test, for foam materials of different permeabilities and thicknesses. Furthermore, an identical glass cube was constructed at NTUA in order to facilitate optical access at KIT where measurements were also performed inside the cube. All of these measurements will become available when data processing is complete, later in the project.

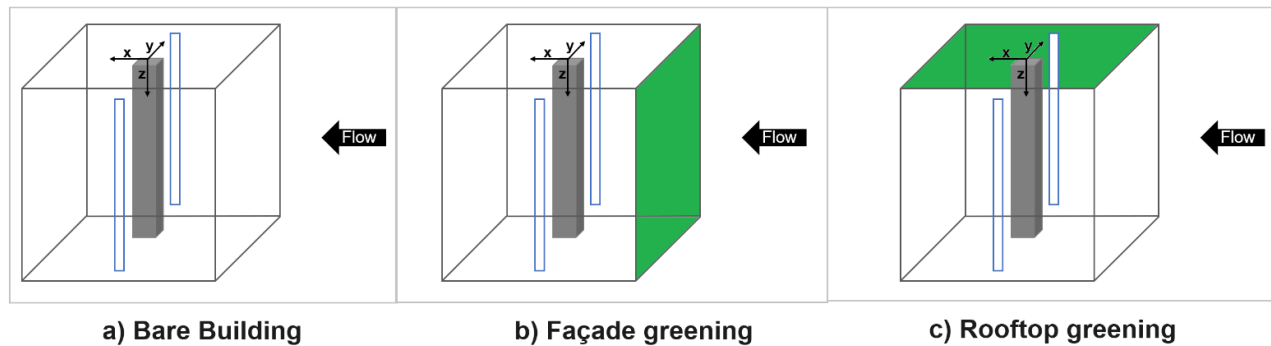**a) Bare Building**   **b) Façade greening**   **c) Rooftop greening**

Figure 22 Tested configurations in both wind tunnels (KIT, NTUA): a) Bare building (without vegetation), b) Façade greening and c) Rooftop greening.

Measurements were performed for all experimental configurations in both KIT and NTUA wind tunnels, at common locations around the building, in order to permit cross comparison of the results. However, the measurements were performed with different experimental measurement techniques: Laser Doppler Anemometry (LDA) at KIT and Particle Image Velocimetry (PIV) at NTUA. Details of the measurement points and the experimental set ups are presented in the following sections.

4.2.1 KIT – LDA measurements

Velocity measurements at KIT were performed with Lased Doppler Velocimetry, which is a pointwise method and involves traversing the space from point to point to position the probe. Measurements were performed along three horizontal profiles on the side wall of the building, upstream and downstream of the opening, along three vertical profiles on the roof and three vertical profiles in the wake. Details of the measurement settings for each are provided following.

For the side wall, the measurement positions are schematically shown in Figure 23. Since LDV is capable of high sampling rates, for the points at close proximity to the side wall, where unsteady flow phenomena and high turbulent velocity fluctuations are expected, lateral velocities were sampled at a higher frequency. Details of the parameters used in the measurements are provided in Table 3

S.W.A: (-0.4H,1H,0.5H)
S.W.B: (-0.2H,1H,0.5H)
S.W.C: (+0.1H,1H,0.5H)
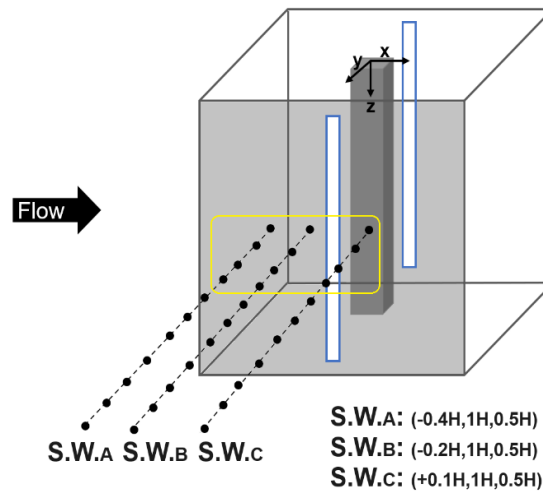
Figure 23 Measurement points' positions on the side wall of the bare building configuration. Black dots correspond to points sampled at a frequency of fsamp = 100 Hz and the yellow box frame corresponds to the area where measurements were sampled with fsamp = 500 Hz.

Table 3 LDV measurement parameters for side wall measurements

Laser Doppler Velocimetry (full range)	
2D velocity measurements	streamwise u & lateral v
Sampling frequency, f_{samp}	100 Hz
Acquisition time, t_{ac}	120 sec
Number of points / configuration	32
Laser Doppler Velocimetry (wall proximity range)	
1D velocity measurements	lateral v
Sampling frequency, fsamp	500 Hz
Acquisition time, t_{ac}	120 sec
Number of points / configuration	12

Similarly, to the side wall, for the roof, the measurement positions are schematically shown in Figure 24. Again, for the points at close proximity to the roof, vertical velocities were sampled at a

higher frequency. Details of the parameters used in the measurements are provided in Table 3 Measurement positions in the wake and the relevant measurement parameters are shown in Figure 25 and Table 5, respectively
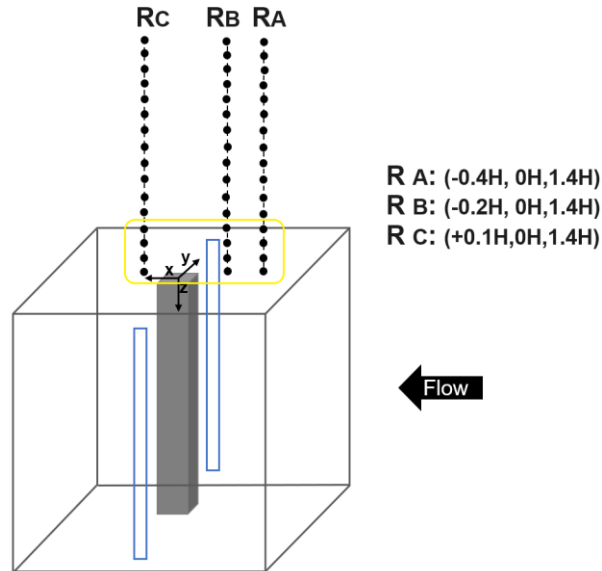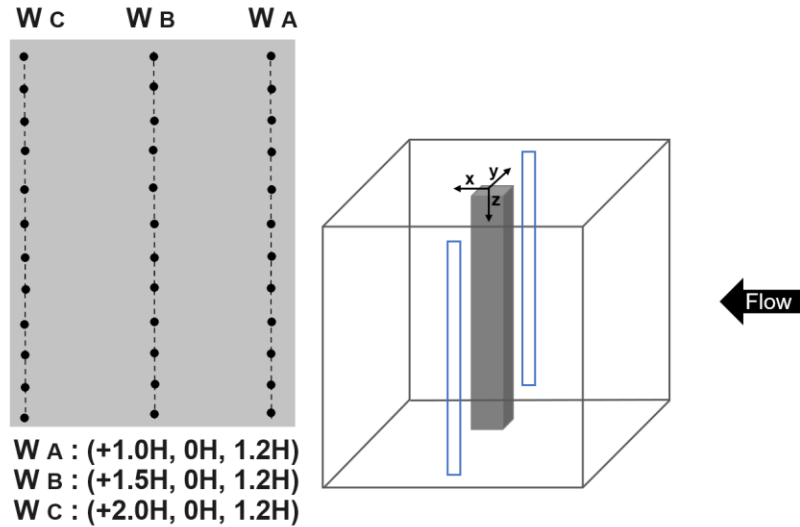

Figure 24 Measurement points' positions on the roof of the bare building configuration. Black dots correspond to points sampled at a frequency of fsamp = 100 Hz and the yellow box frame corresponds to the area where measurements were sampled with fsamp = 500 Hz.

Table 4 LDV measurement parameters for measurements on the roof

Laser Doppler Velocimetry (full range)	
2D velocity measurements	streamwise u & vertical w
Sampling frequency, f_{samp}	100 Hz
Acquisition time, t_{ac}	120 sec
Number of points / configuration	48
Laser Doppler Velocimetry (wall proximity range)	
1D velocity measurements	vertical w
Sampling frequency, fsamp	500 Hz
Acquisition time, t_{ac}	120 sec
Number of points / configuration	12

Figure 25. Measurement points' positions in the wake of the bare building configuration.

Table 5 LDV measurement parameters for measurements in the wake

Laser Doppler Velocimetry (Wake I)	
2D velocity measurements	streamwise u & vertical w
Sampling frequency, f_{samp}	100 Hz
Acquisition time, t_{ac}	120 sec
Number of points / configuration	36

4.2.2 NTUA – PIV measurements

At NTUA, the velocity measurements were performed with Particle Image Velocimetry (PIV) in both 2D-2C and 2D-3C modes. The PIV method measures on a plane and these were chosen to include the LDV measurement position at KIT. Measurements were performed on three different planes, a horizontal one next to the side wall, a vertical one on the roof and a vertical plane in the wake, behind the building.

For the side wall, the camera was mounted over the building and the laser sheet was directed horizontally towards the side wall at half the building height (z/H=0.5) (Figure 26). A 2D-2C PIV setup was chosen for this plane since a) suspension and alignment of two cameras was difficult to achieve reliably with the available infrastructure and b) the vertical velocity (in the z direction) was not expected to be significant. Parameters relevant to the setup are presented in Table 6.
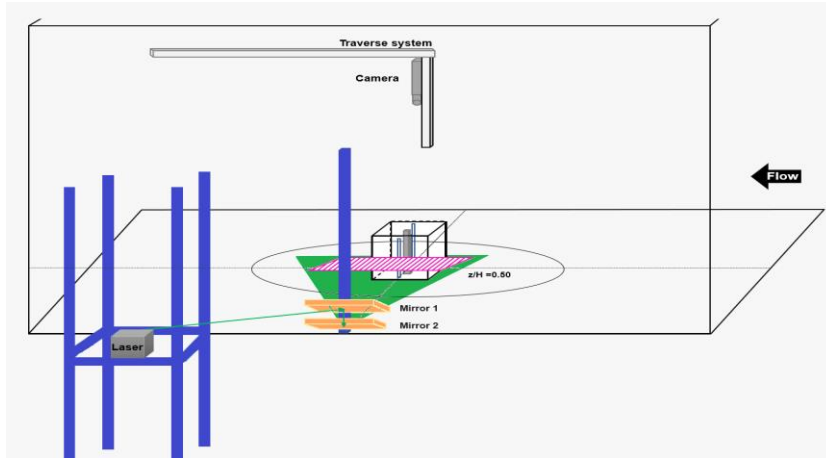
Figure 26 Mono PIV experimental set up of the Side Wall measurement plane (Horizontal Plane).

Table 6 Measurement parameters for the 2D-2C PIV measurements on the horizontal side wall plane

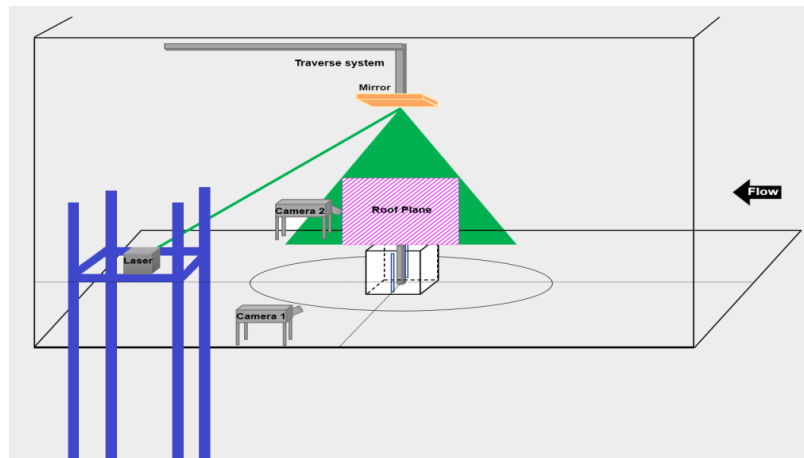| Mono (2D – 2 component) Particle Image Velocimetry (2D-2C PIV)	
2D velocity measurements	streamwise u & lateral v
Angle of attack (AoA)	0^0
Parameter	Horizontal Plane
Plane orientation with respect to free stream	Normal
Plane Size	1.82H × 1.82H
Sampling frequency, f_{samp}	7.28 Hz
Lenses	90 mm
Distance from measured plane	12.36 H
Interrogation area size	32 px
Interrogation area size	1.61 mm
Minimum resolvable velocity	0.095 m/s
Minimum resolvable velocity (normalized with respect to the free stream)	1.9%
Number of snapshots per plane	1000

For the measurements in the wake and on the roof, a 2D-3C setup was chosen as the cameras could be placed on the floor of the wind tunnel, significantly alleviating difficulties appearing in the overhead suspension of the horizontal setup.

For measurement of the vertical plane above the roof, the cameras were slightly elevated in order to achieve optical access above the building and a horizontally oriented angle plane between the two cameras (Figure 27). The laser sheet was redirected to the vertical direction with a mirror suspended above the model. For the vertical plane in the wake, the cameras were positioned downstream and on either side of the building model, in order to ensure optical access to the area directly behind the building. Redirection of the laser sheet was achieved in the same manner as for the roof plane (Table 7). Details of the measurement parameters for both vertical planes are given in Table 7.

Co-funded by the European Union

4. Twin Test #1: Effects of Vegetation on Flows in the Urban Environment
4.2 Experimental Configurations and Settings   *45*

Table 7 Measurement parameters for the 2D-3C PIV measurements on the vertical planes above the roof and in the wake

Stereo (2D – 3 component) Particle Image Velocimetry (2D-3C, Stereo PIV)		
3D velocity measurements	streamwise u & lateral v & vertical w	
Angle of attack (AoA)	0^0	
Parameter	Roof Plane	Wake Plane
Plane orientation with respect to free stream	Parallel	Parallel
Plane Size	1.82H × 1.82H	
Sampling frequency, f_{samp}	7.28 Hz	
Lenses	150 mm	150 mm
Camera contained angle	90^0	90^0
Distance from measured plane	15.45 H	15.45 H
Interrogation area size	32 px	32 px
Interrogation area size	1.72 mm	1.66 mm
Minimum resolvable velocity	0.10 m/s	0.10 m/s
Minimum resolvable velocity (normalized with respect to the free stream)	2%	2%
Number of snapshots per plane	1000	1000

Figure 27. Stereo PIV experimental set up of the Roof measurement plane.

4. Twin Test #1: Effects of Vegetation on Flows in the Urban Environment
4.2 Experimental Configurations and Settings
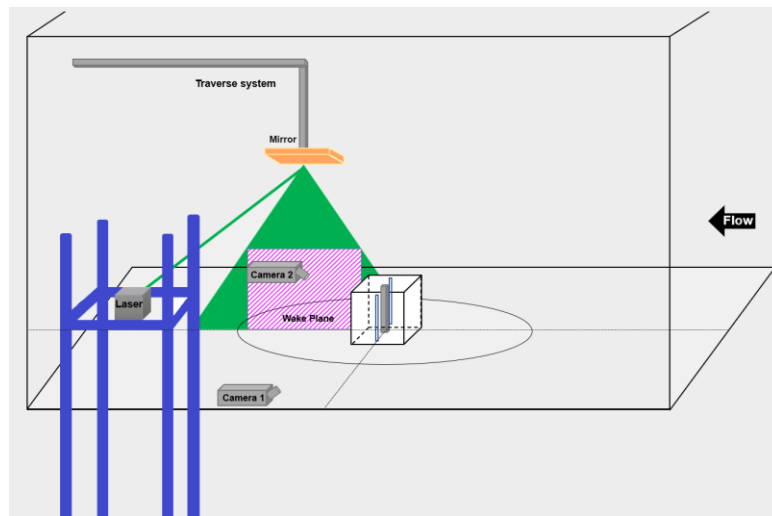
Figure 28 Stereo PIV experimental set up of the Wake measurement plane.

4. Twin Test #1: Effects of Vegetation on Flows in the Urban Environment
4.2 Experimental Configurations and Settings

4.3 Measurement Results

4.3.1 Comparison of KIT and NTUA measurements

Results from the measurements in the KIT and NTUA wind tunnels are presented here. A comparison of the two wind tunnel measurements/measurement techniques is presented first for the profiles on the side wall, the roof and in the wake. These include the mean values for the two velocity components measured both at KIT and NTUA, as well as the values of the standard deviations of these velocity components.

Following, the effect of placing vegetation on either the upstream face or the roof is presented, again for both measurement techniques.
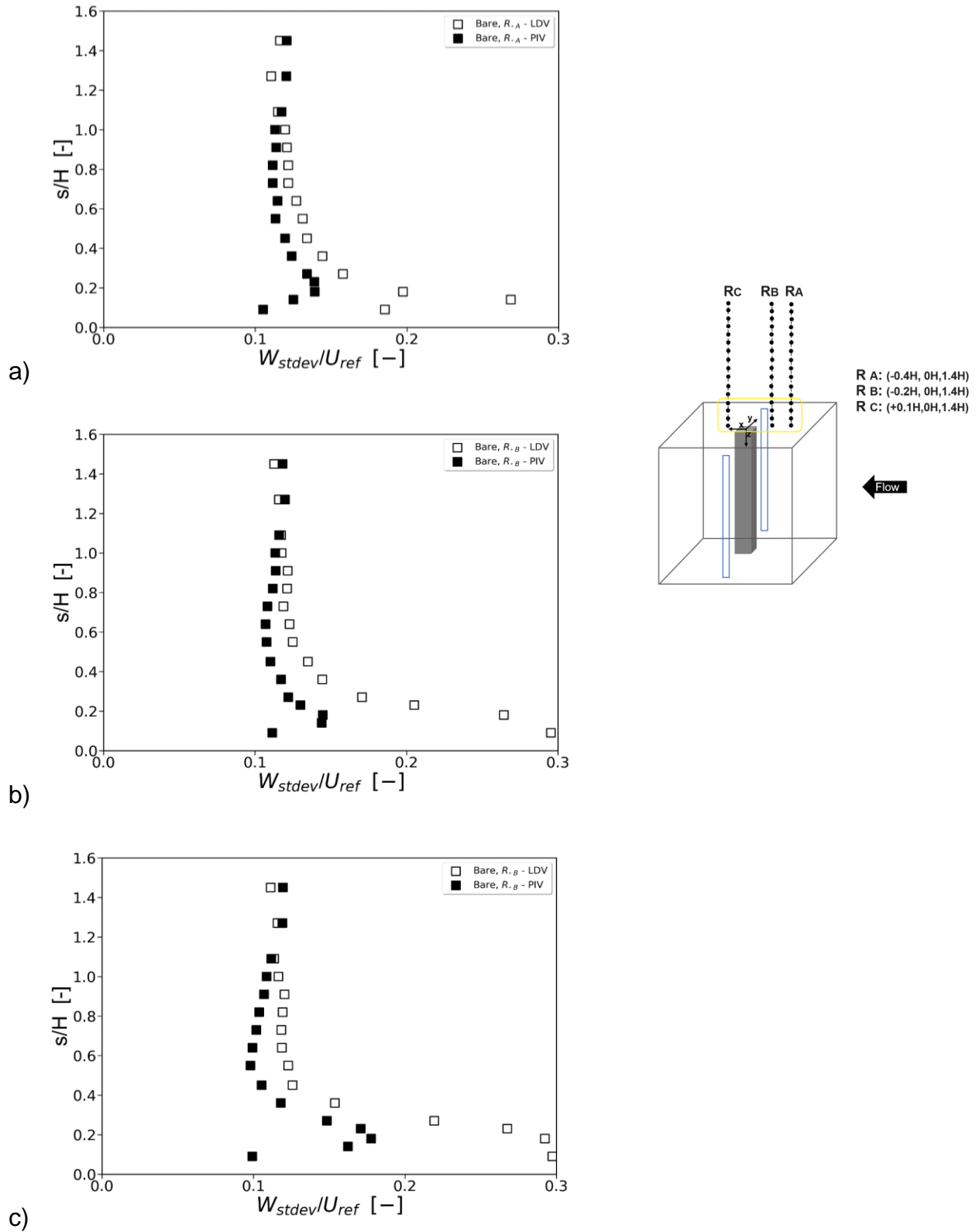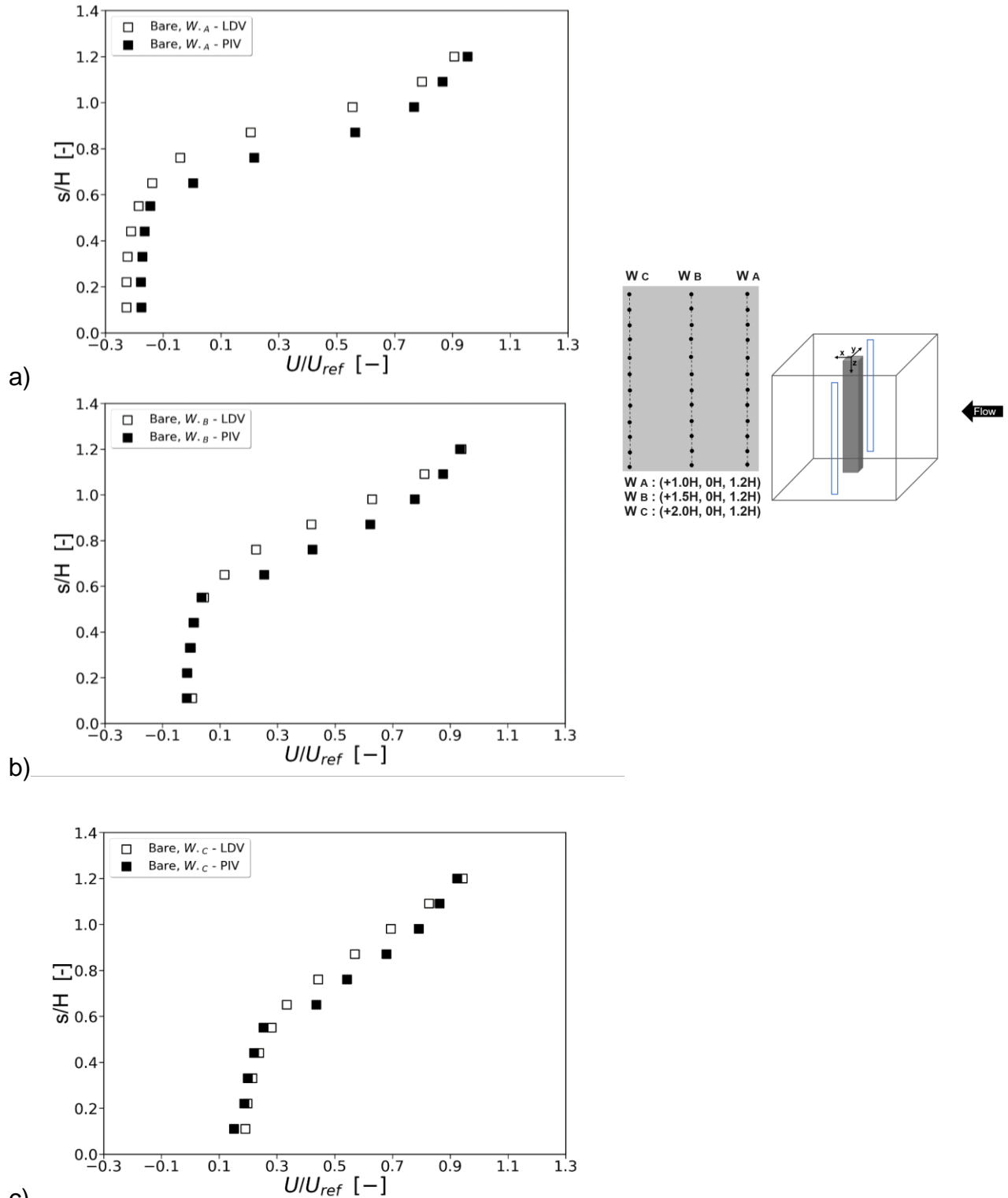
4.3.1.1 Side Wall

a)

b)

c)
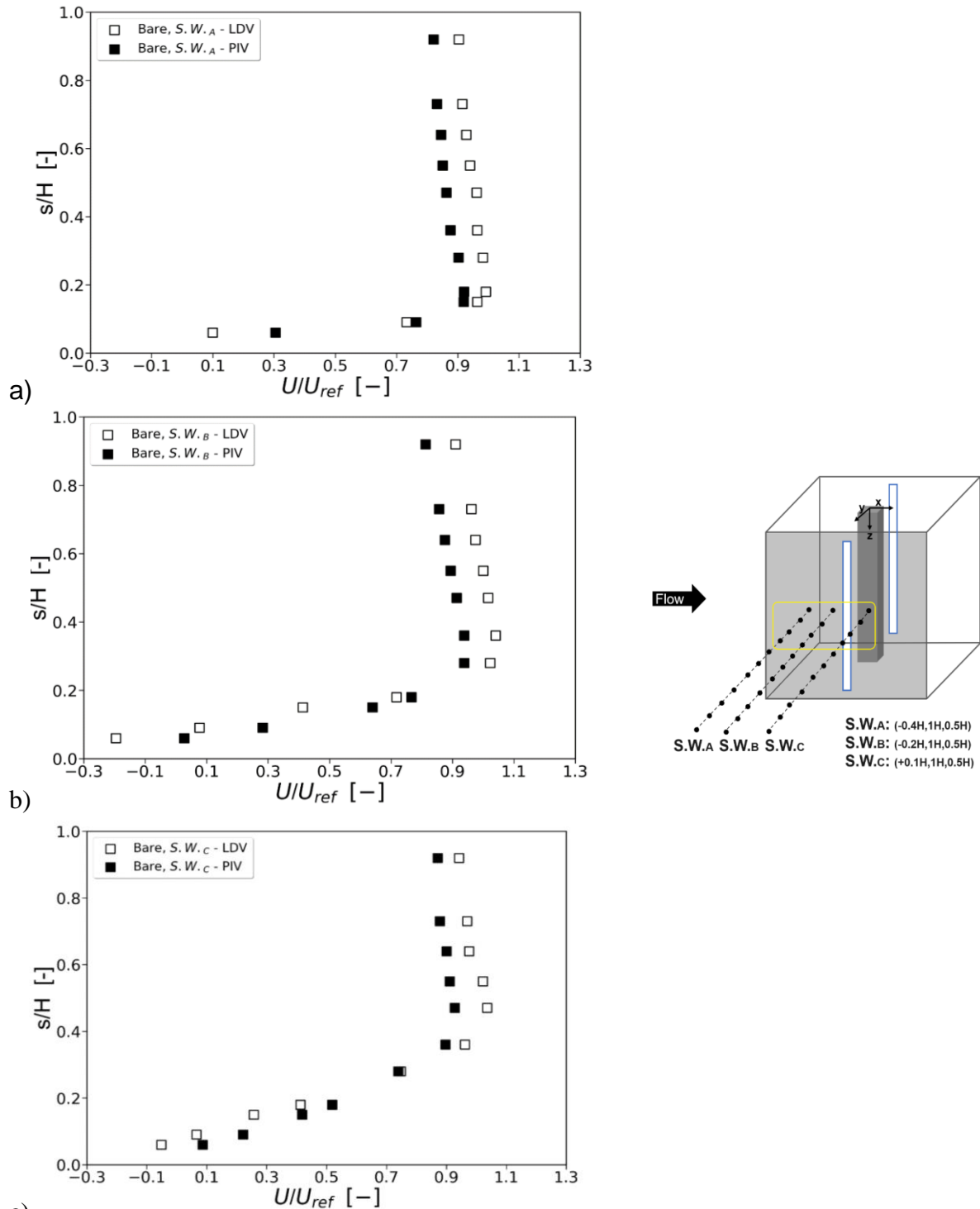
Figure 29. Non-dimensional mean streamwise velocity profiles of LDV measurements at KIT (white square) and Mono PIV measurements at NTUA (black square), on the side wall at a) (S.W. a), b) (S.W. b) , c) (S.W. C) for the Bare building configuration.
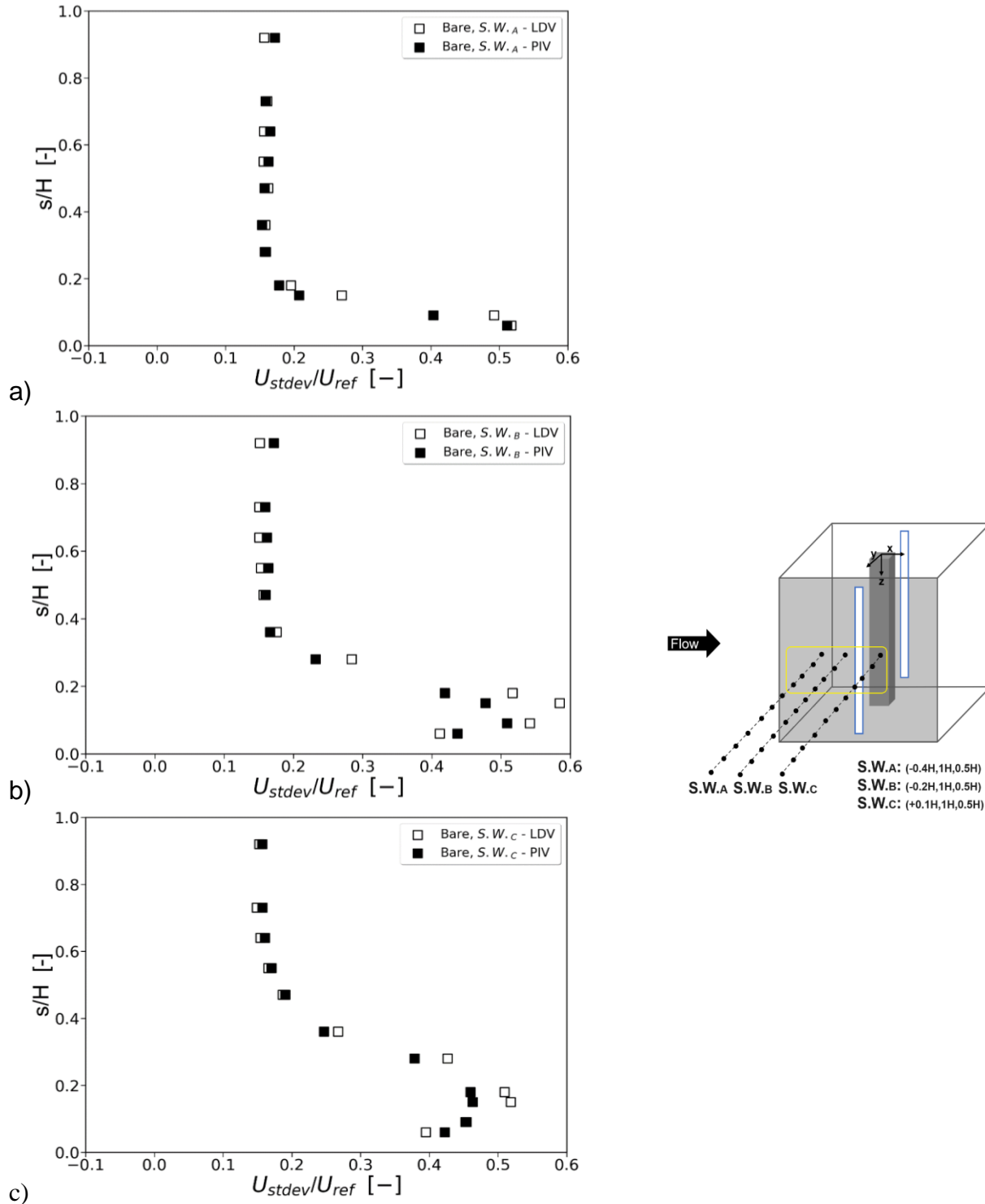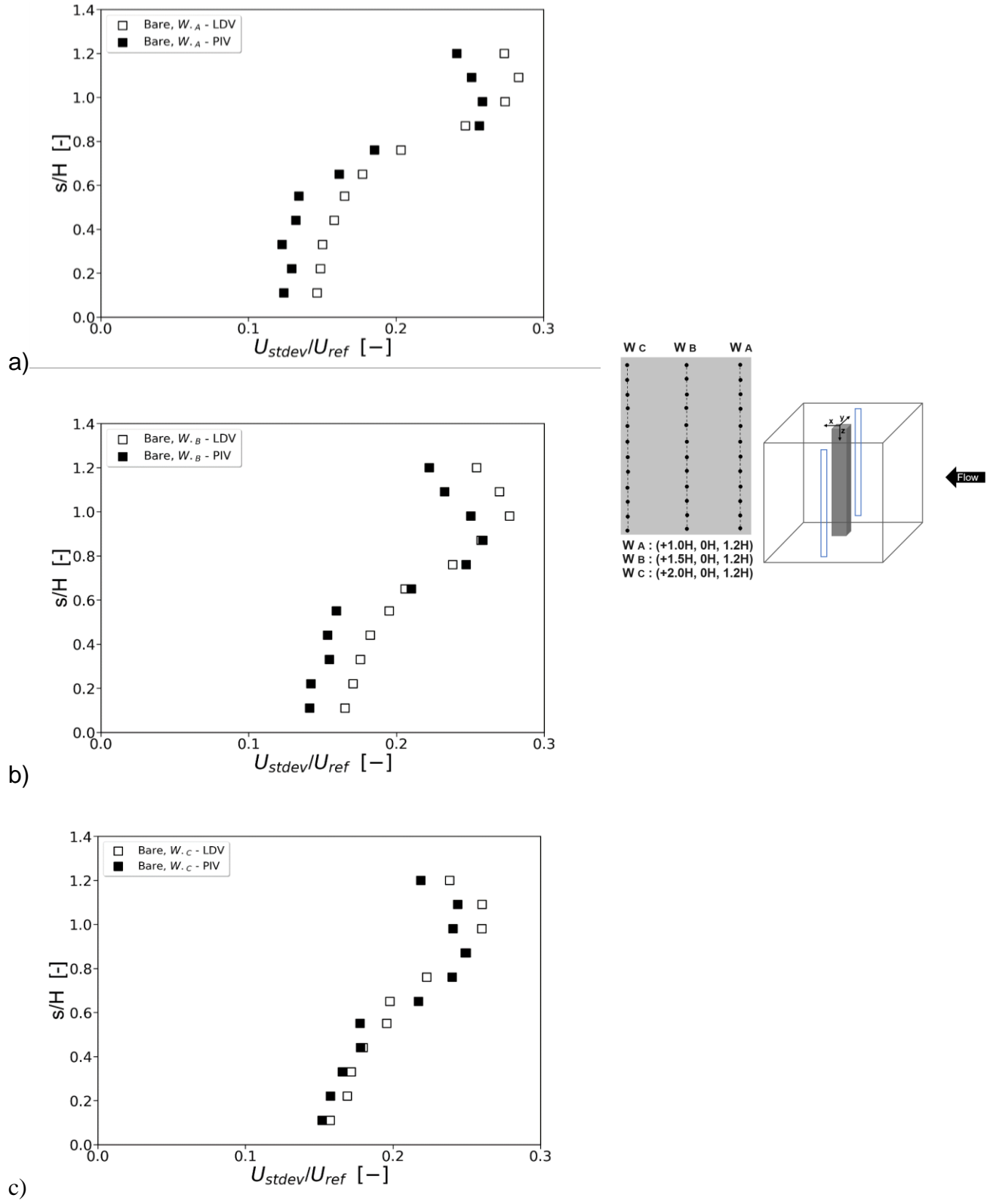
Figure 30. Non-dimensional stdev streamwise velocity profiles of LDV measurements at KIT (white square) and Mono PIV measurements at NTUA (black square), on the side wall at a) (S.W. a), b) (S.W. b) , c) (S.W. C) for the Bare building configuration.

a)

b)

c)
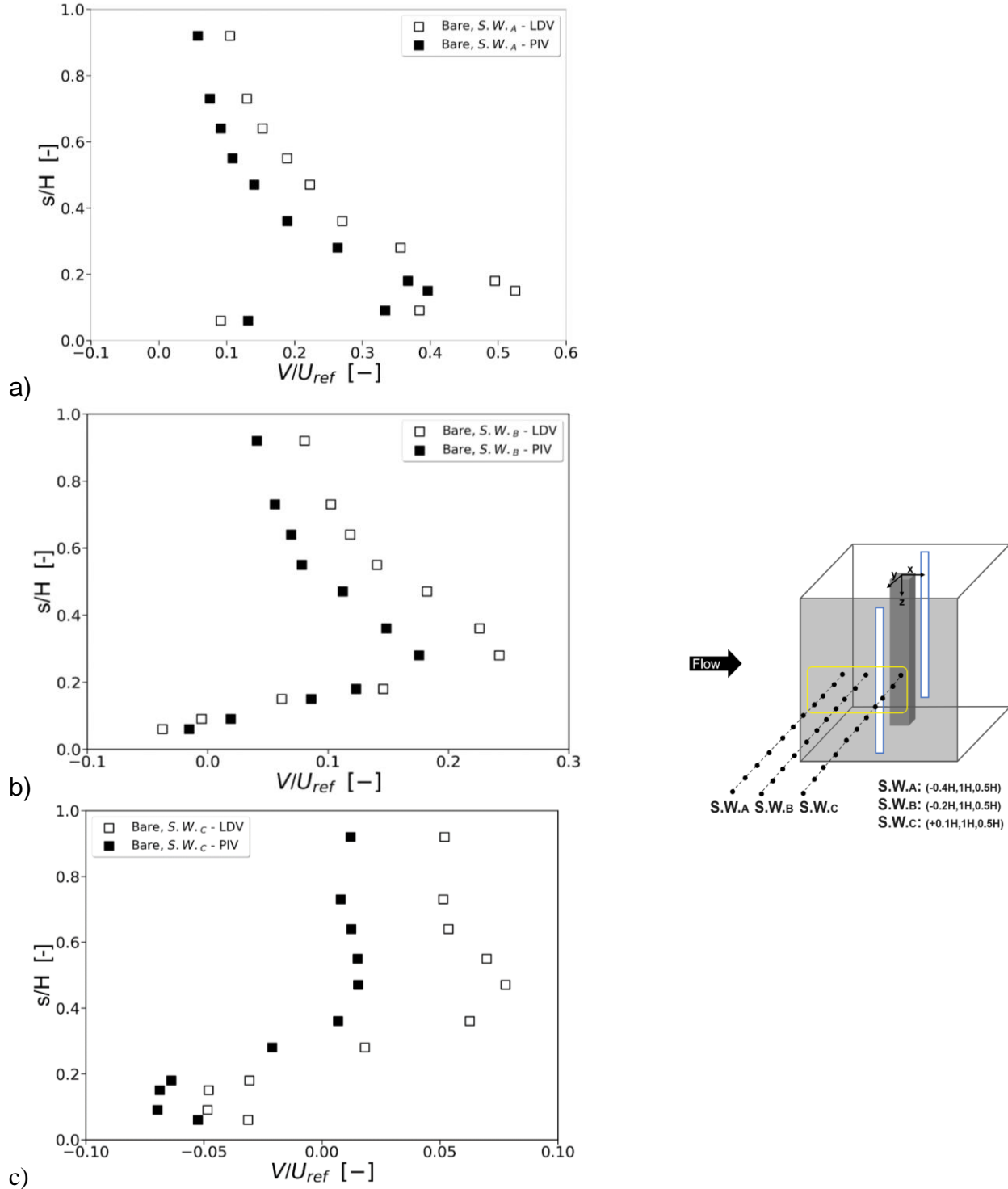
Figure 31. Non-dimensional mean lateral velocity profiles of LDV measurements at KIT (white square) and Mono PIV measurements at NTUA (black square), on the side wall at a) (S.W. a), b) (S.W. b) , c) (S.W. c) for the Bare building configuration.
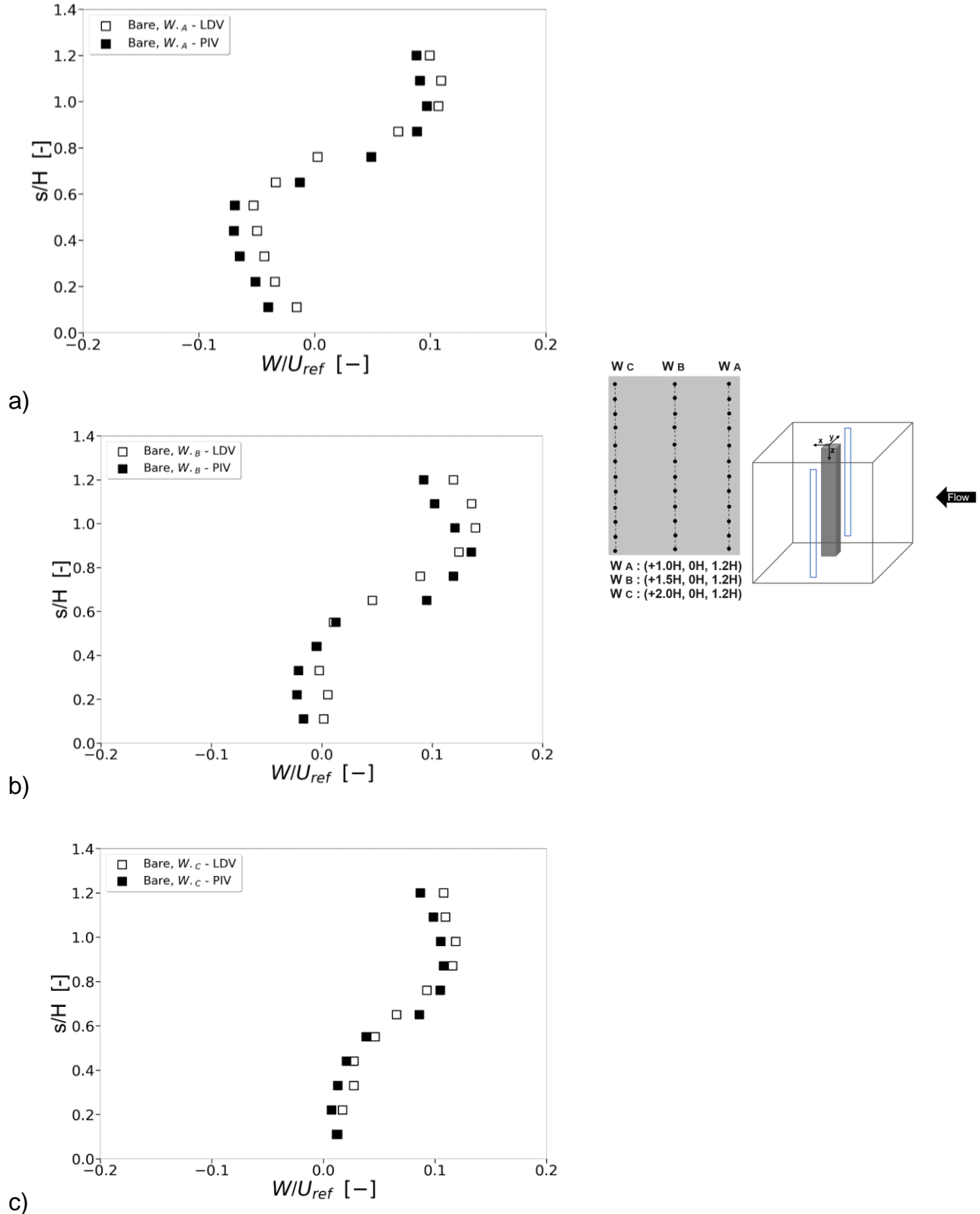
a)

b)

c)
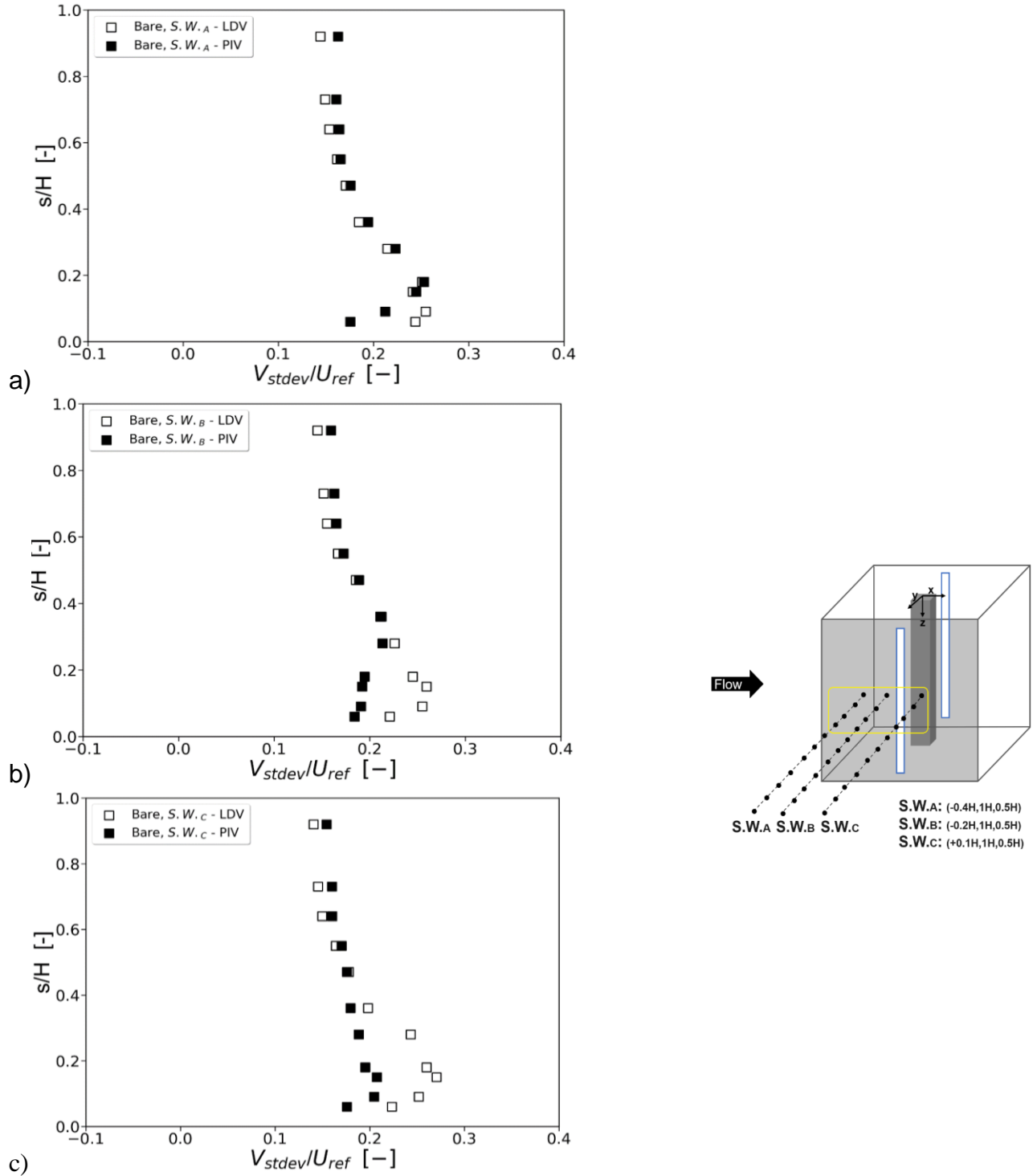
Figure 32 Non-dimensional stdev lateral velocity profiles of LDV measurements at KIT (white square) and Mono PIV measurements at NTUA (black square), on the side wall at a) (S.W. a), b) (S.W. b) , c) (S.W. C) for the Bare building configuration.

4.3.1.2 Roof

a)

b)

c)
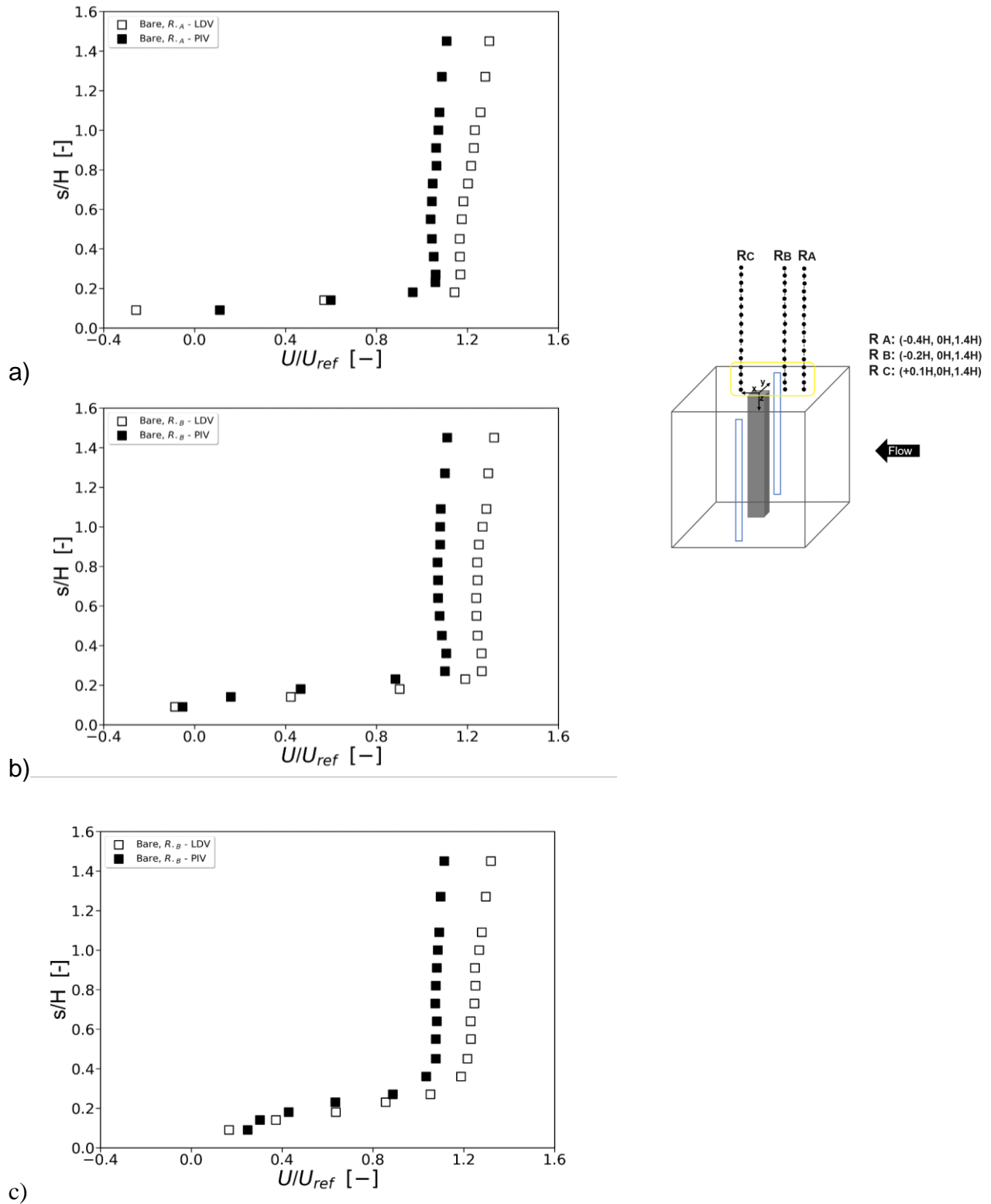
Figure 33 Non-dimensional mean streamwise velocity profiles of LDV measurements at KIT (white square) and Stereo PIV measurements at NTUA (black square), on the roof a) (R. a) b) (R. b) c) (R. c) for the Bare building configuration.
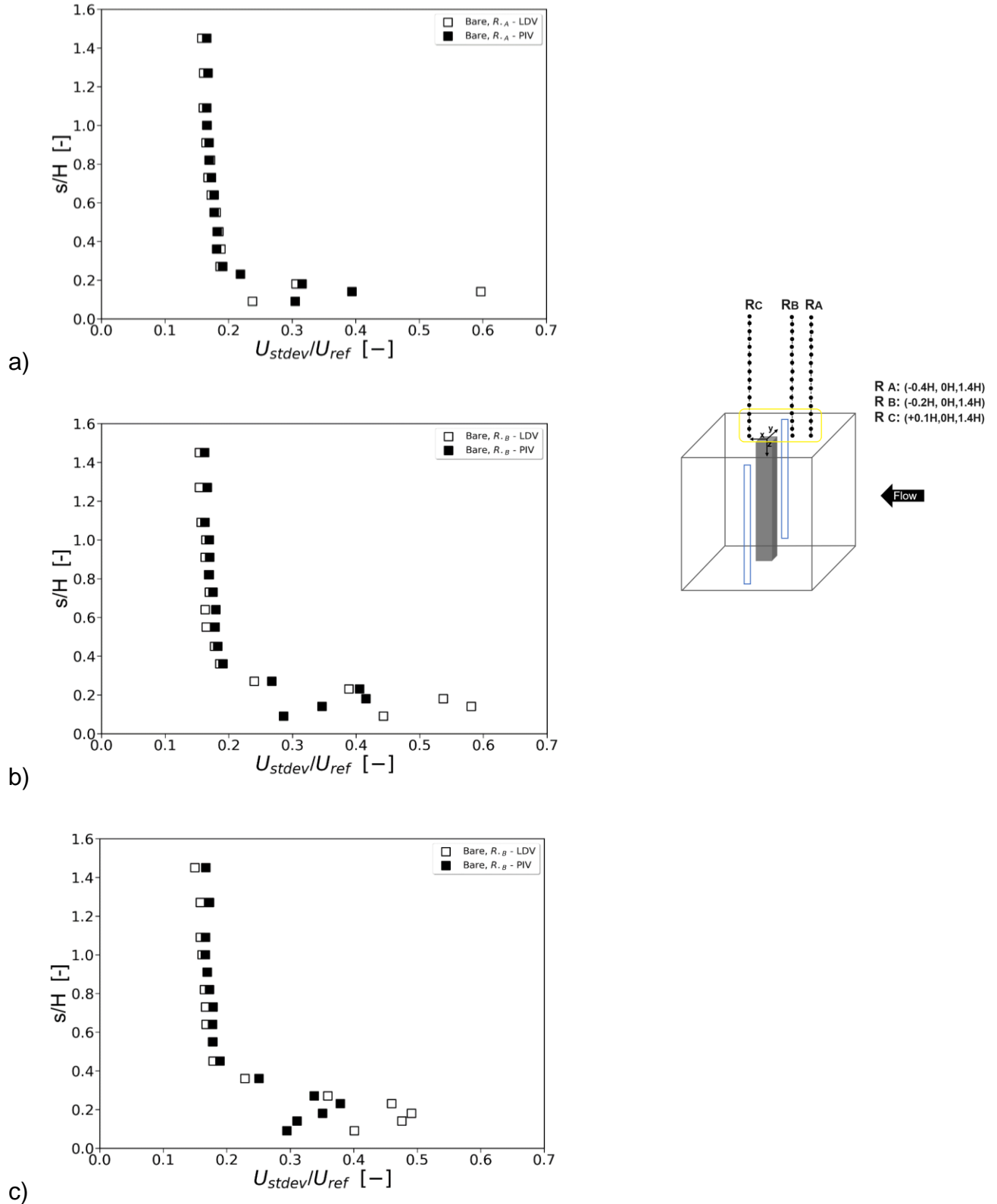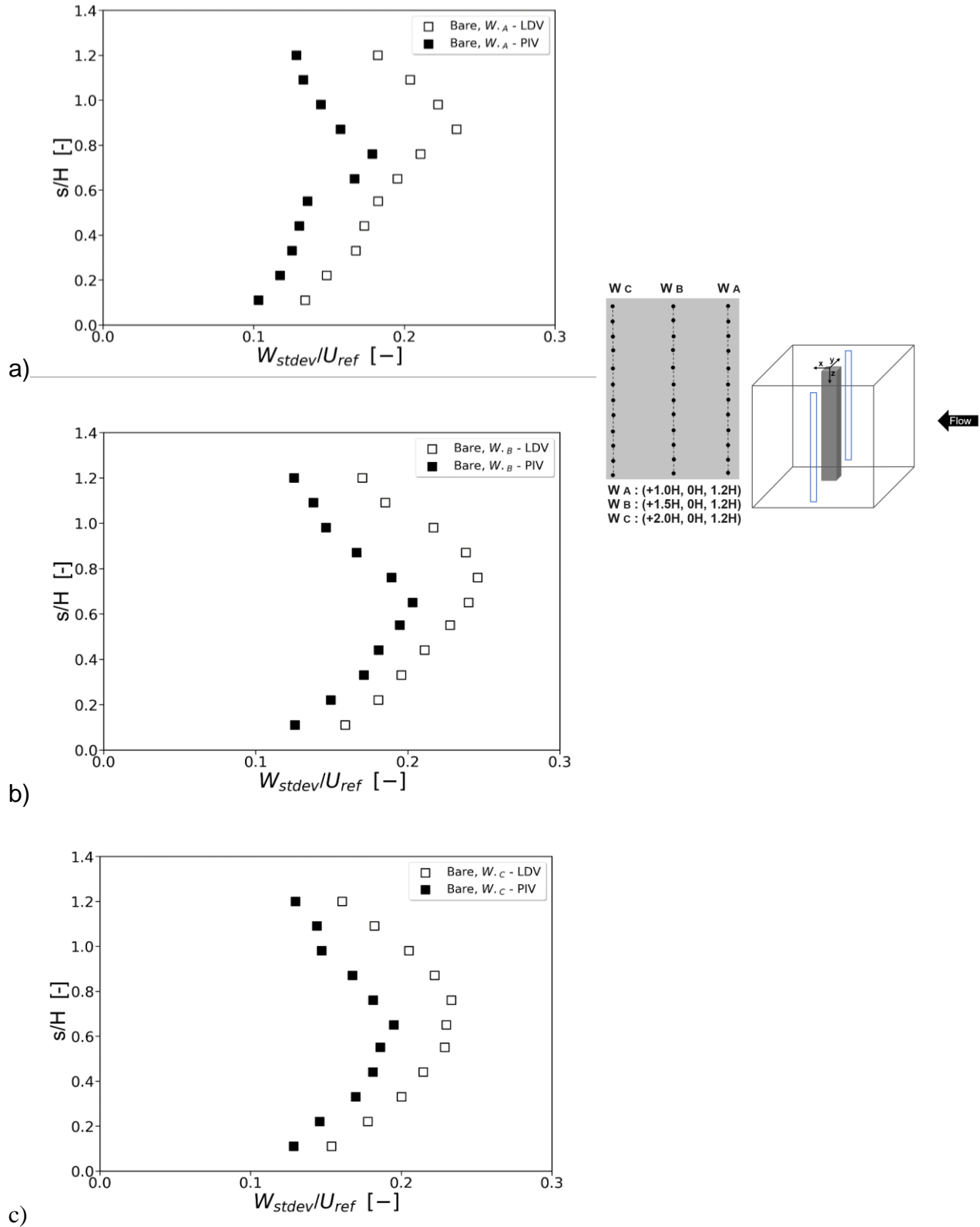
Figure 34. Non-dimensional stdev streamwise velocity profiles of LDV measurements at KIT (white square) and Stereo PIV measurements at NTUA (black square), on the roof a) (R. a) b) (R. b) c) (R. c) for the Bare building configuration
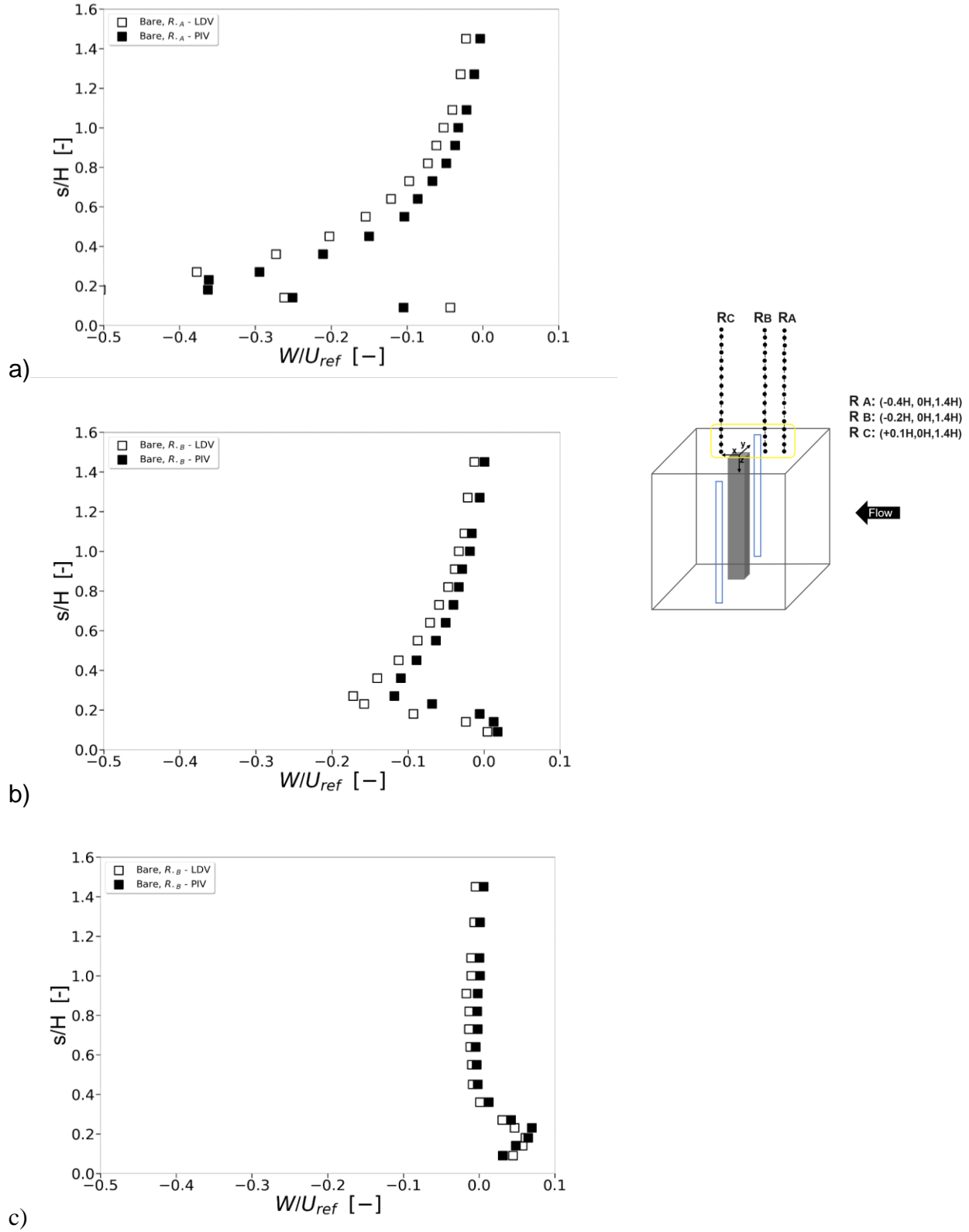
Figure 35. Non-dimensional mean vertical velocity profiles of LDV measurements at KIT (white square) and Stereo PIV measurements at NTUA (black square), on the roof a) (R. a) b) (R. b) c) (R. c) for the Bare building configuration

a)

b)

c)

Figure 36 Non-dimensional stdev vertical velocity profiles of LDV measurements at KIT (white square) and Stereo PIV measurements at NTUA (black square), on the roof a) (R. a) b) (R. b) c) (R. c) for the Bare building configuration

4. Twin Test #1: Effects of Vegetation on Flows in the Urban Environment
4.3 Measurement Results

4.3.1.3 Wake

a)

b)

c)

Figure 37 Non-dimensional mean streamwise velocity profiles of LDV measurements at KIT (white square) and Stereo PIV measurements at NTUA (black square), on the roof a) (R. a) b) (R. b) c) (R. c) for the Bare building configuration

Figure 38. Non-dimensional stdev streamwise velocity profiles of LDV measurements at KIT (white square) and Stereo PIV measurements at NTUA (black square), on the roof a) (R. a) b) (R. b) c) (R. c) for the Bare building configuration

a)

b)

c)

Figure 39. Non-dimensional mean vertical velocity profiles of LDV measurements at KIT (white square) and Stereo PIV measurements at NTUA (black square), on the roof a) (R. a) b) (R. b) c) (R. c) for the Bare building configuration

Figure 40 Non-dimensional stdev vertical velocity profiles of LDV measurements at KIT (white square) and Stereo PIV measurements at NTUA (black square), on the roof a) (R. a) b) (R. b) c) (R. c) for the Bare building configuration

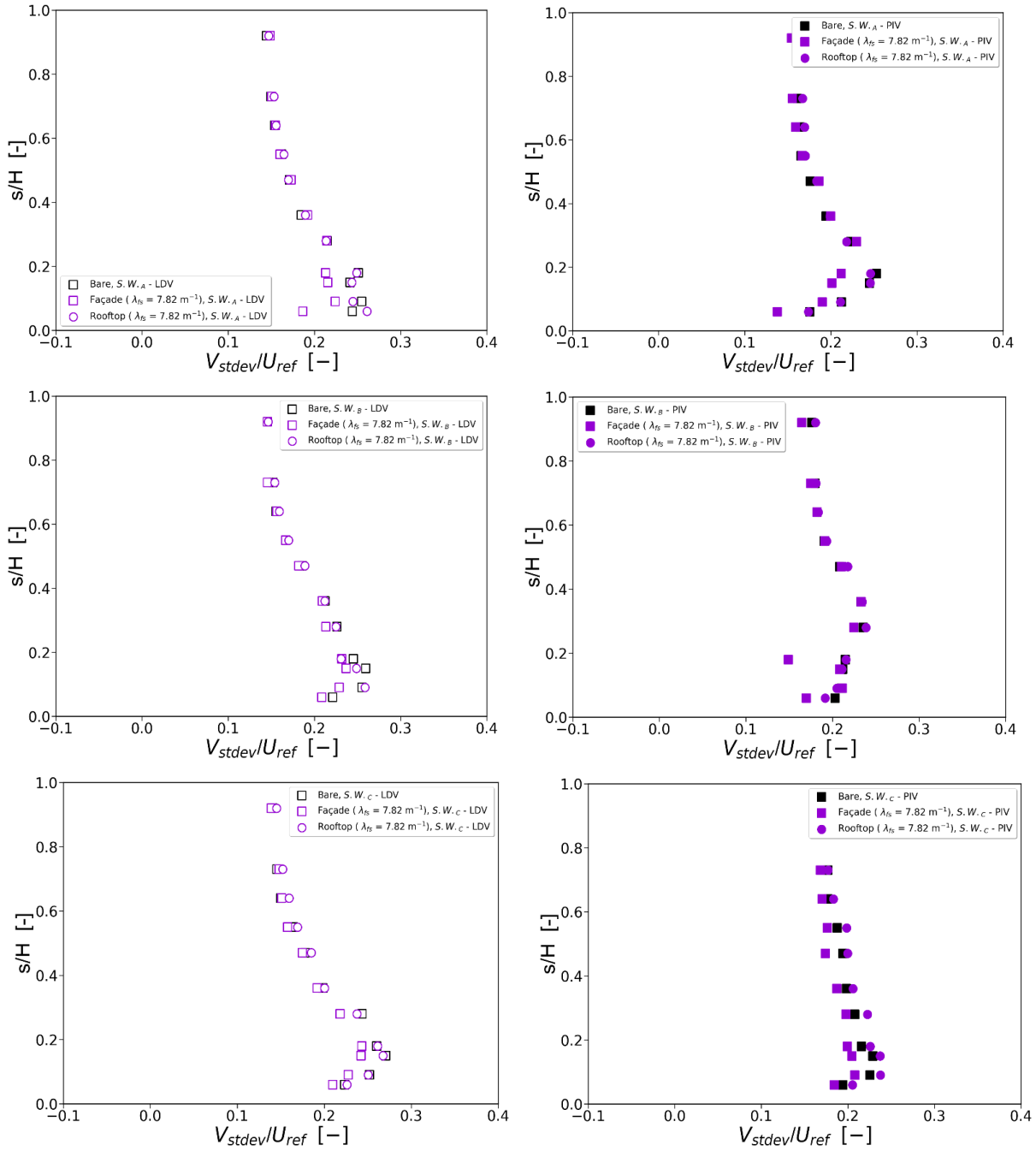## 4.3.2 Effects of Vegetation

4.3.2.1 Side Wall

a)

b)

c)
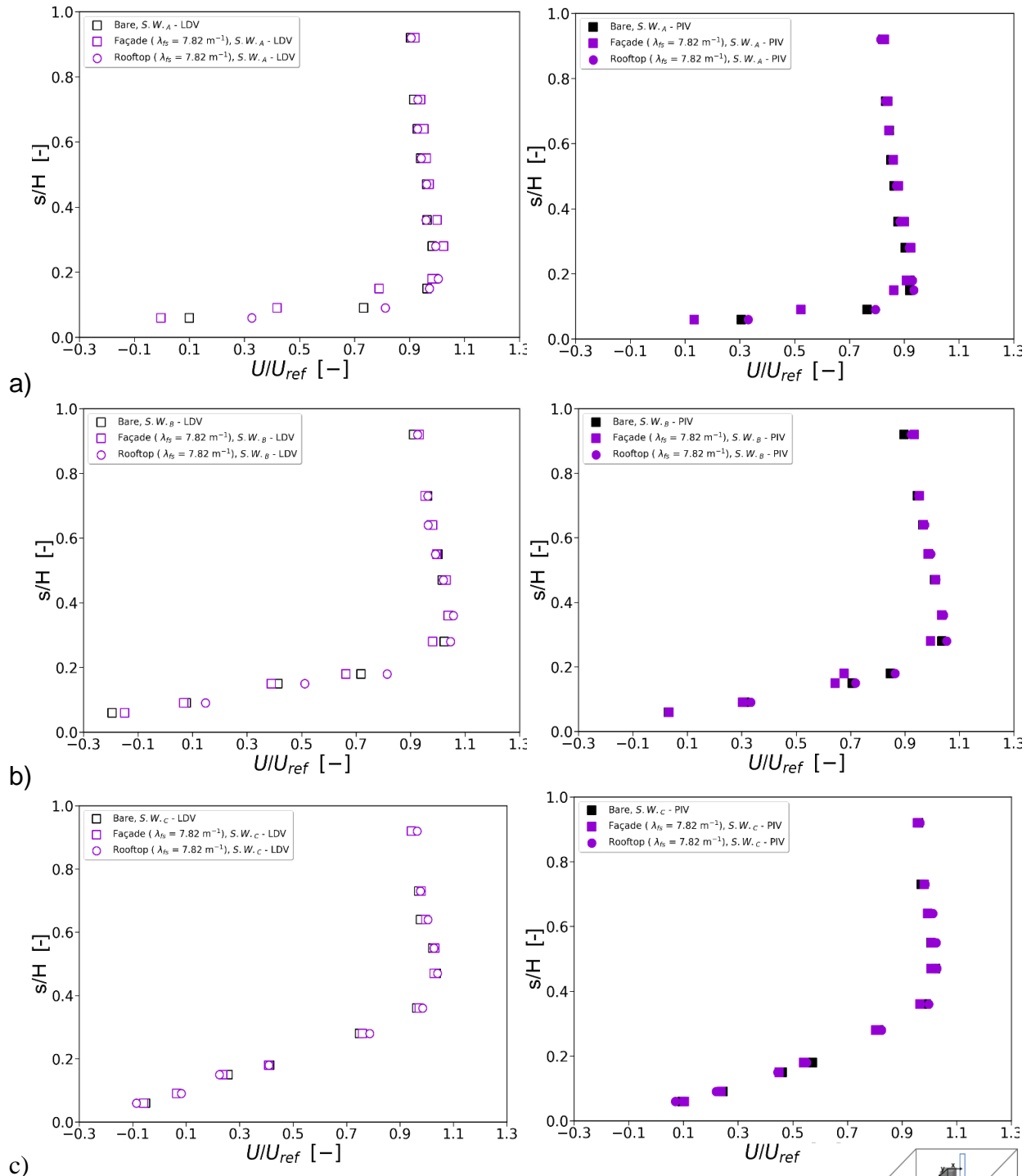
Figure 41 Non-dimensional mean streamwise velocity profiles of LDV (left) and PIV (right) for: Bare building (black square), Façade greening (purple square), Rooftop greening (purple circle) on the side wall at a) (S.W. a), b) (S.W. b) , c) (S.W. C)

4. Twin Test #1: Effects of Vegetation on Flows in the Urban Environment
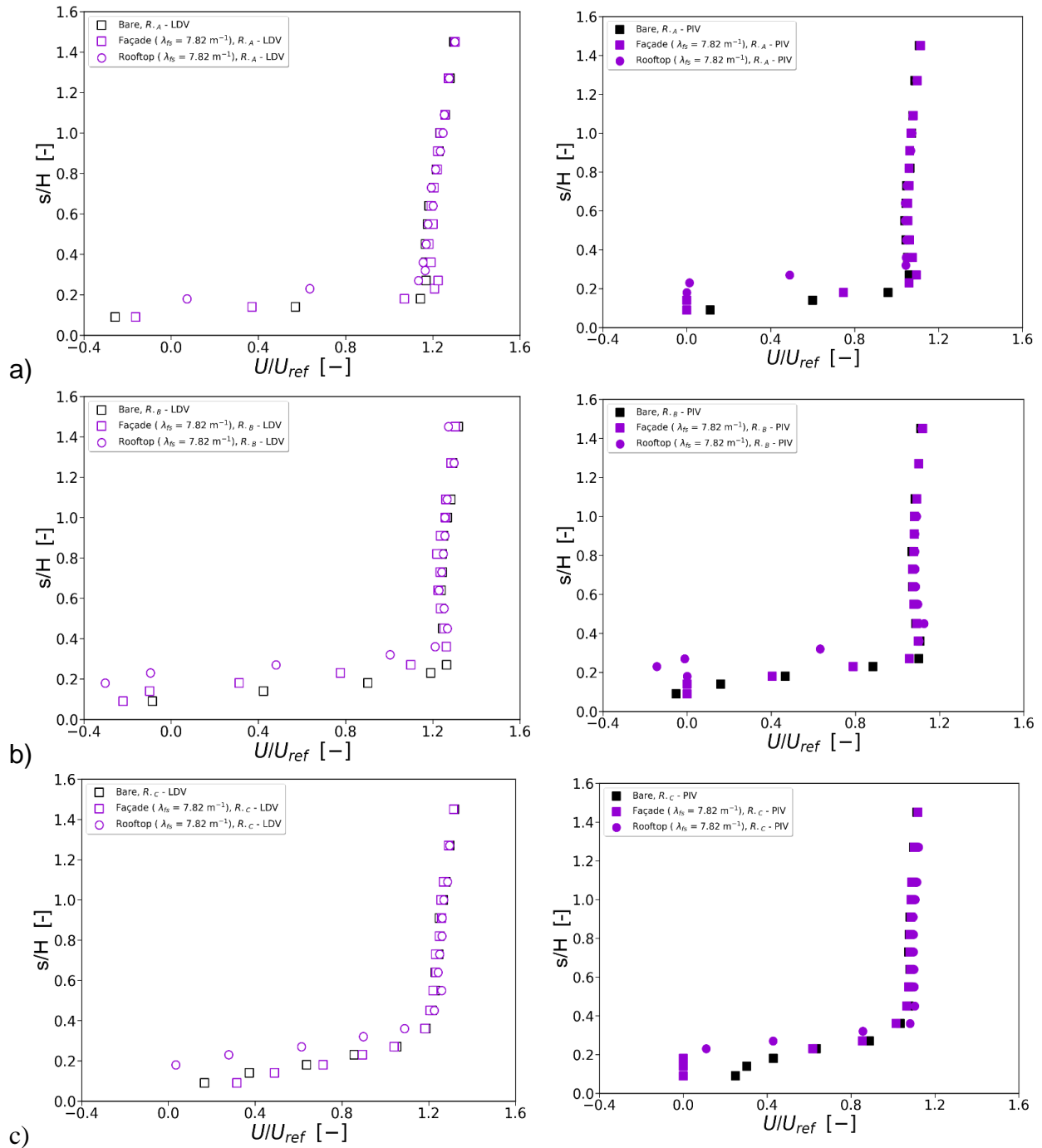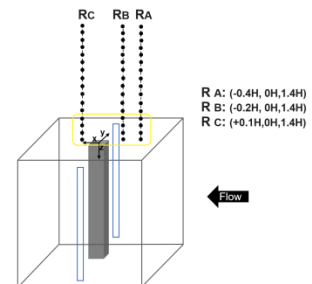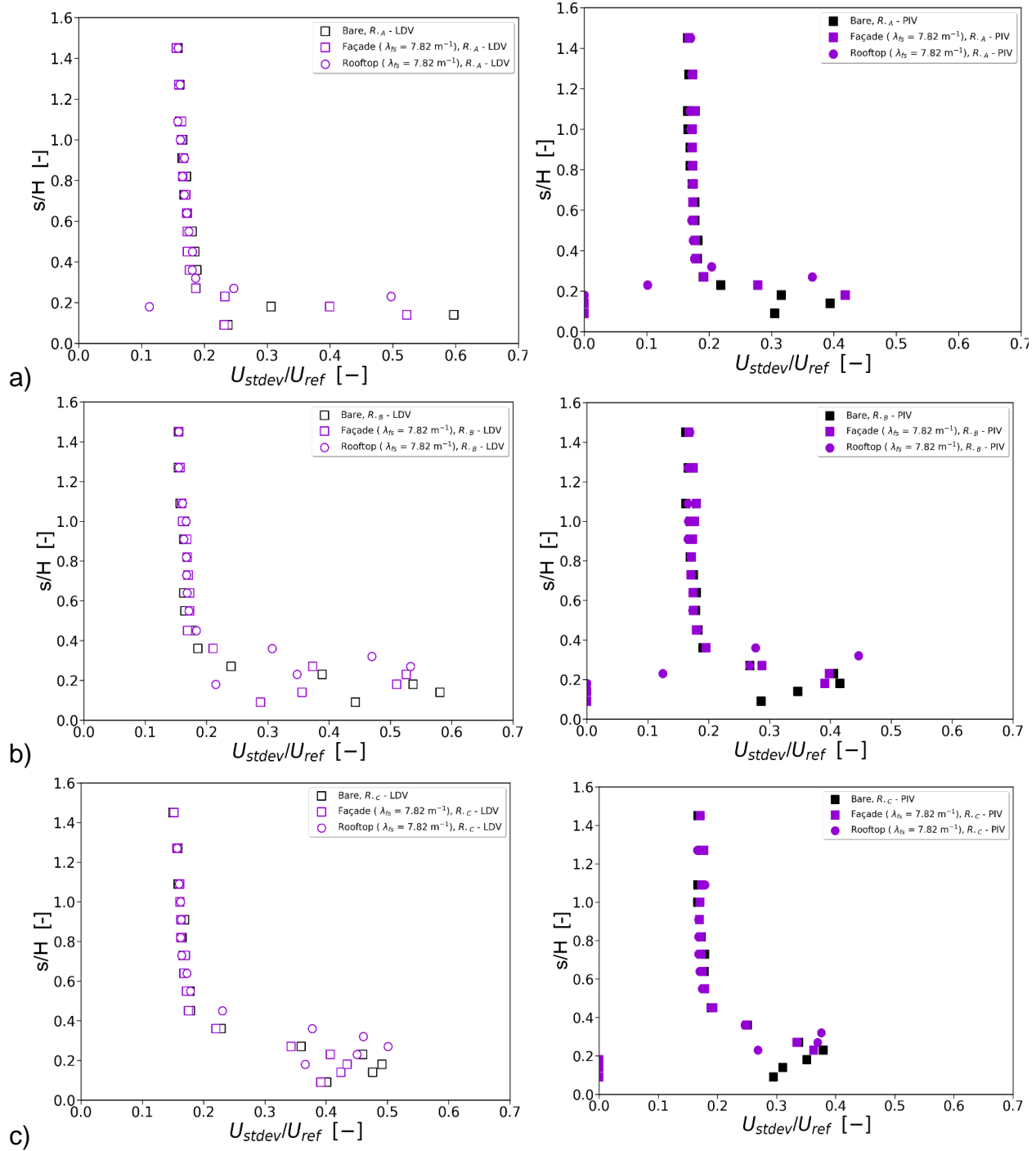*4.3 Measurement Results*
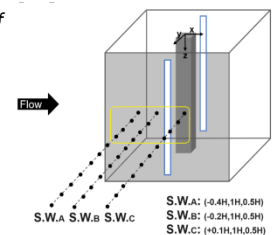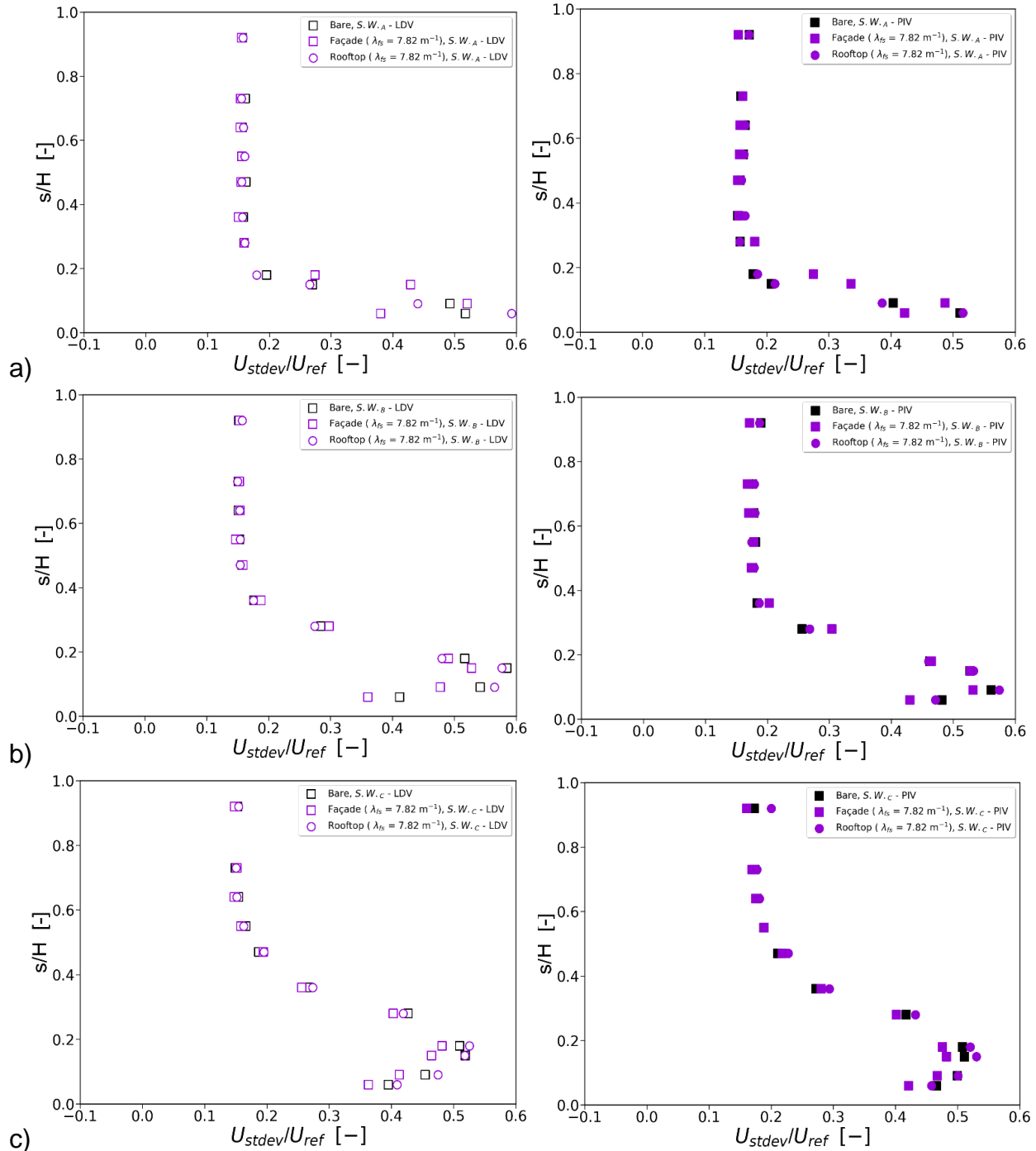
Figure 42 Non-dimensional stdev streamwise velocity profiles of LDV (left) and PIV (right) for: Bare building (black square), Façade greening (purple square), Rooftop greening (purple circle) on the side wall at a) (S.W. a), b) (S.W. b) , c) (S.W. C)
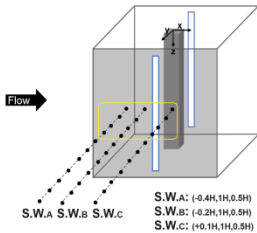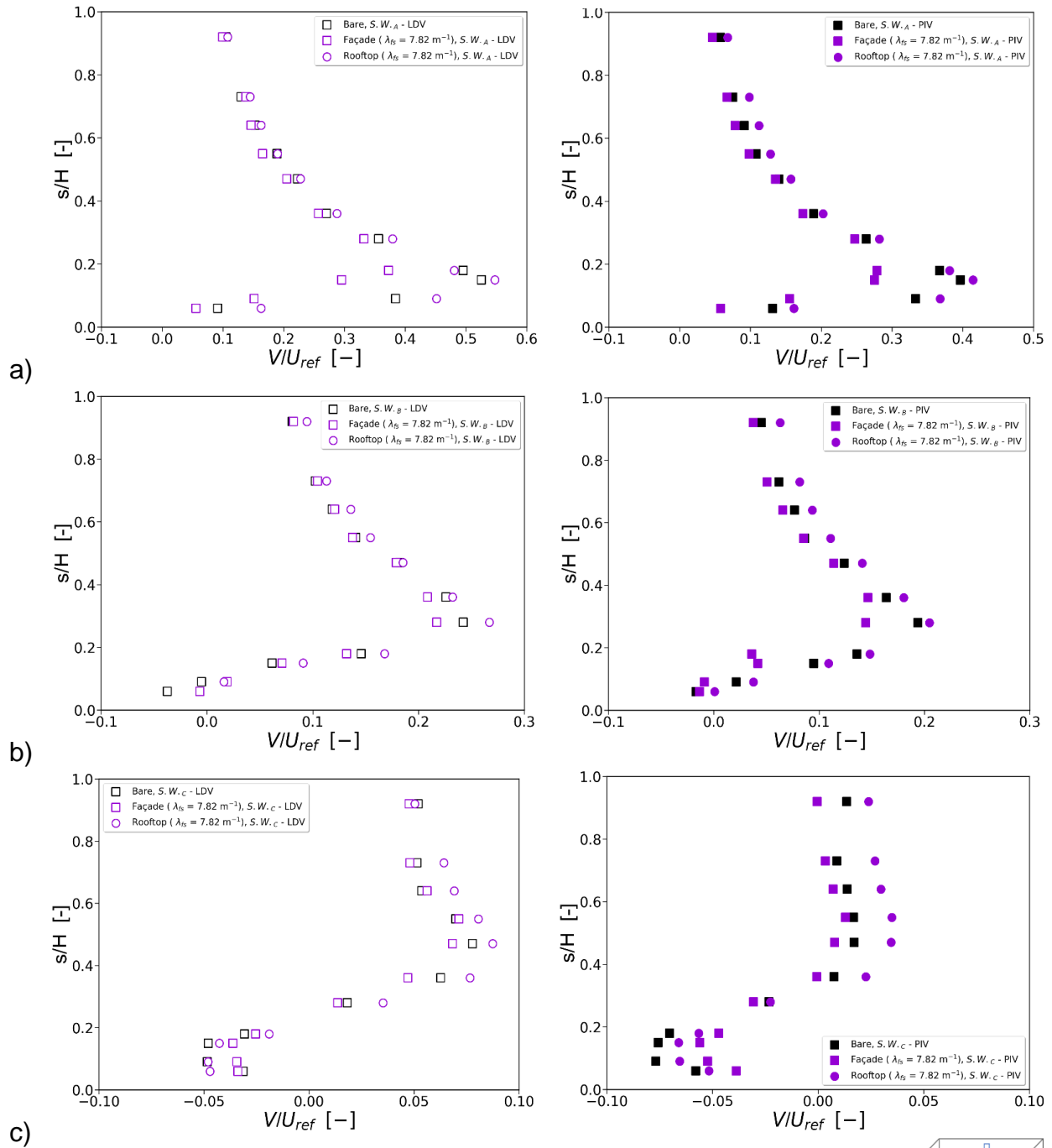
Figure 43 Non-dimensional mean lateral velocity profiles of LDV (left) and PIV (right) for: Bare building (black square), Façade greening (purple square), Rooftop greening (purple circle) on the side wall at a) (S.W. a), b) (S.W. b) , c) (S.W. C)
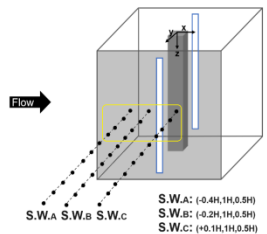
Figure 44 Non-dimensional stdev lateral velocity profiles of LDV (left) and PIV (right) for: Bare building (black square), Façade greening (purple square), Rooftop greening (purple circle) on the side wall at a) (S.W. a), b) (S.W. b) , c) (S.W. C)
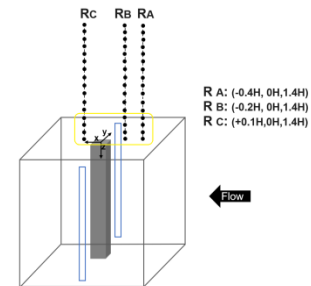
4.3.2.2 Roof

a)

b)

c)
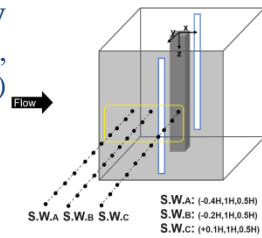
Figure 45 Non-dimensional mean streamwise velocity profiles of LDV (left) and PIV (right) for: Bare building (black square), Façade greening (purple square), Rooftop greening (purple circle) on the roof at a) (R a), b) (R b) , c) (R $_C$)

R A: (-0.4H, 0H, 1.4H)
R B: (-0.2H, 0H, 1.4H)
R C: (+0.1H, 0H, 1.4H)

Figure 46 Non-dimensional stdev streamwise velocity profiles of LDV (left) and PIV (right) for: Bare building (black square), Façade greening (purple square), Rooftop greening (purple circle) on the roof at a) (R a), b) (R b) , c) (R. $_C$)
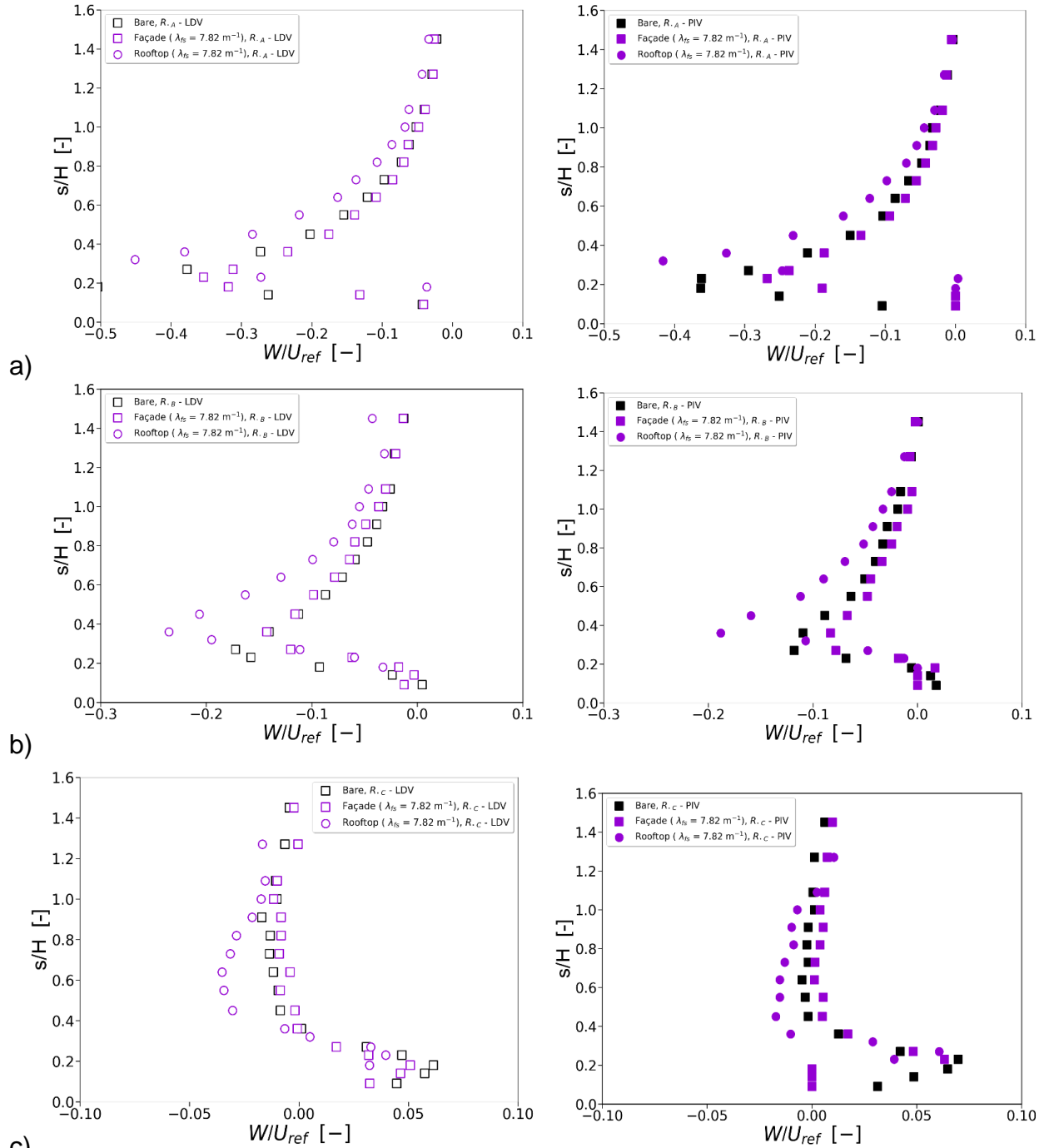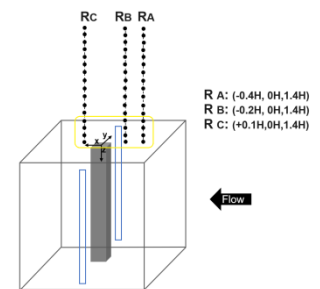
Figure 47 Non-dimensional mean vertical velocity profiles of LDV (left) and PIV (right) for: Bare building (black square), Façade greening (purple square), Rooftop greening (purple circle) on the roof at a) (R a), b) (R b) , c) (R. C)
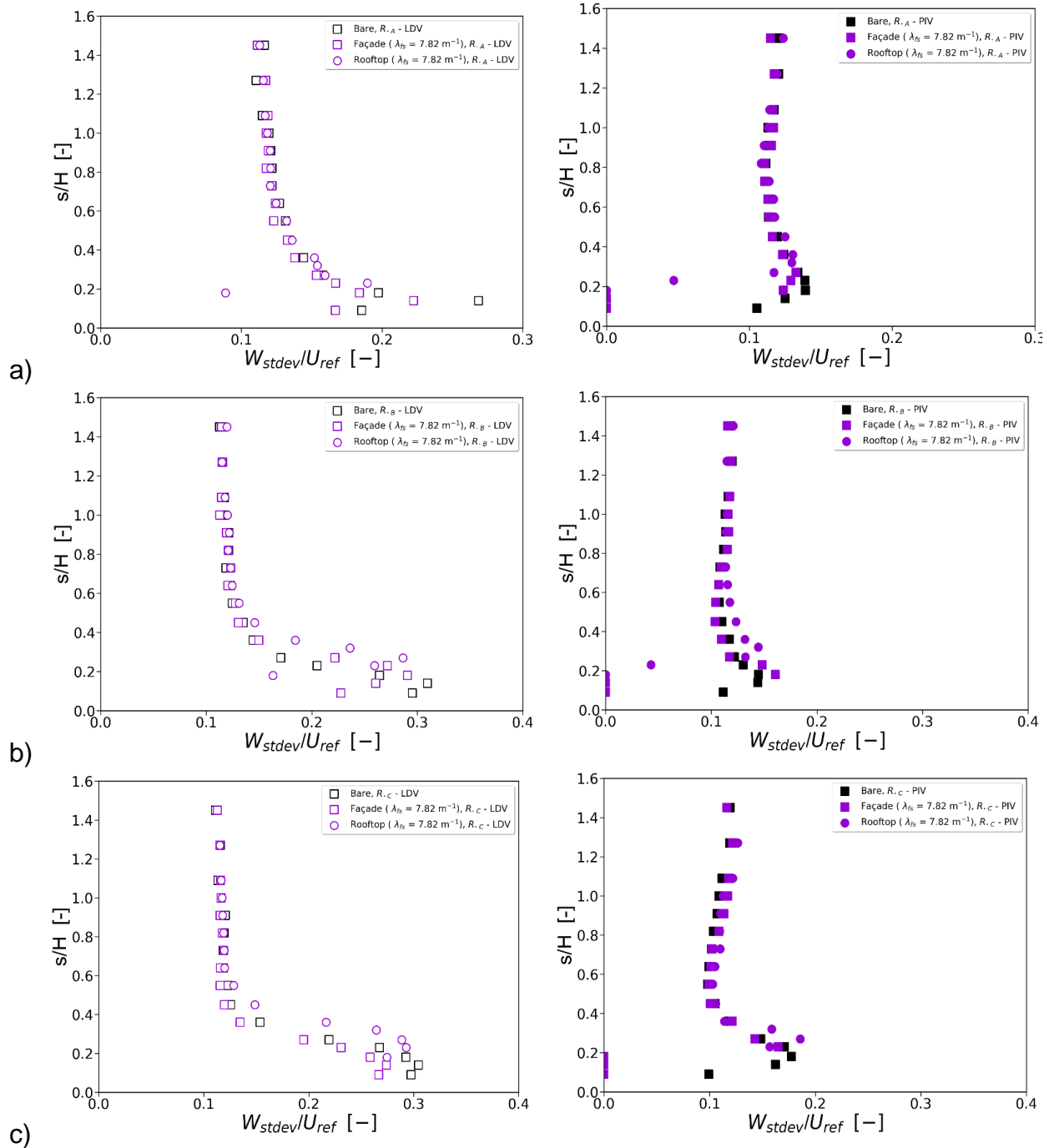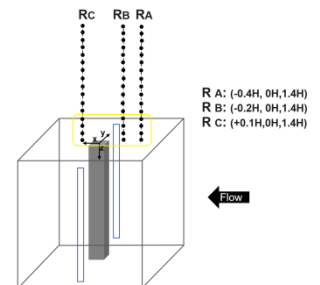
Figure 48 Non-dimensional stdev vertical velocity profiles of LDV (left) and PIV (right) for: Bare building (black square), Façade greening (purple square), Rooftop greening (purple circle) on the roof at a) (R a), b) (R b) , c) (R. $_C$)

4.3.2.3 Wake

4. Twin Test #1: Effects of Vegetation on Flows in the Urban Environment
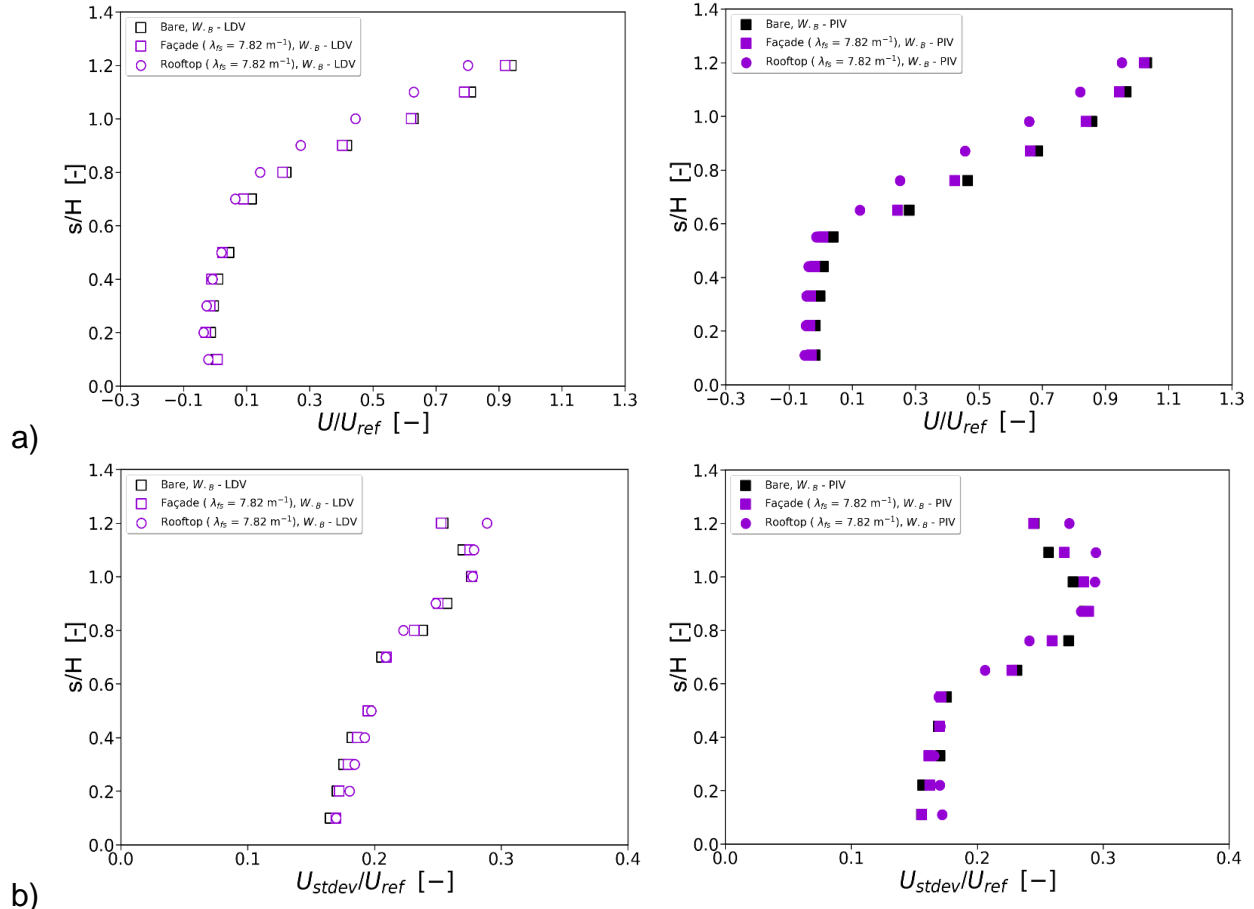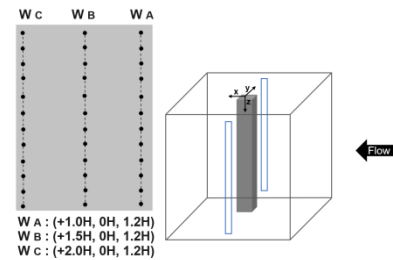*4.3 Measurement Results*

69

Figure 49 Non-dimensional a) mean and b) stdev streamwise velocity profiles of LDV (left) and PIV (right) for: Bare building (black square), Façade greening (purple square), Rooftop greening (purple circle) in the wake at (W $_B$)
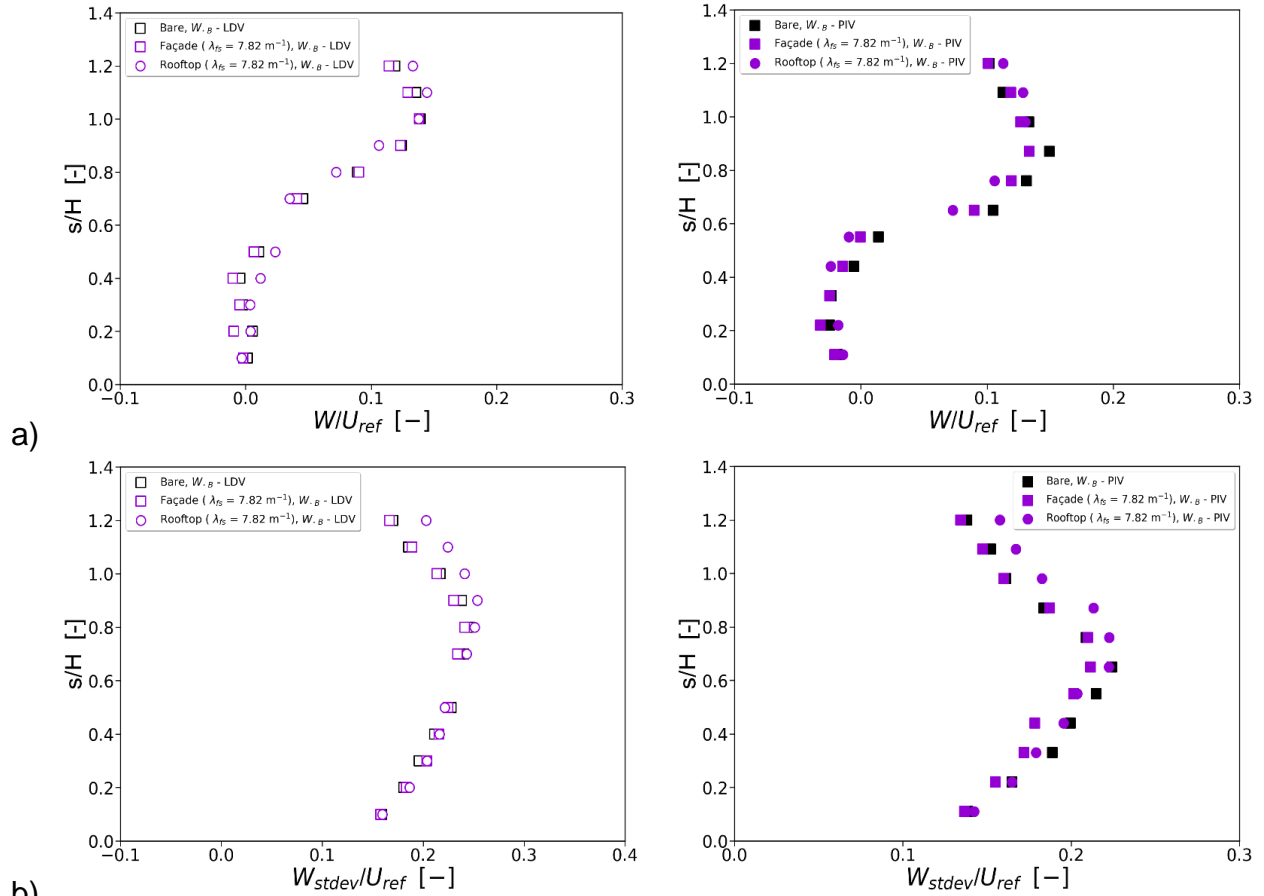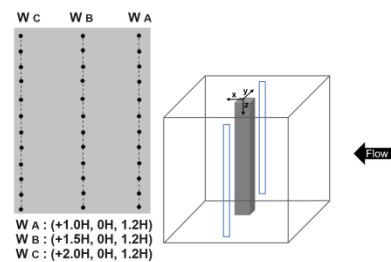
a)

b)

Figure 50 Non-dimensional a) mean and b) stdev vertical velocity profiles of LDV (left) and PIV (right) for: Bare building (black square), Façade greening (purple square), Rooftop greening (purple circle) in the wake at (W $_B$)

5 References

[1] F. Durst, A. Melling, James H. Whitelaw (1976) Principles and Practice of Laser-Doppler Anemometry, Academic Press, 1976 - Fluid dynamic measurements - 405 pages.

[2] H.-E. Albrecht, M. Borys, N. Damaschke, C. Tropea (2003) Laser Doppler and Phase Doppler Measurement Techniques, Springer, 738 pages.

[3] B. Ruck (1987) Laser Doppler Anemometry – a non-intrusive optical measuring technique for fluid velocity, Particle and Particle Systems Characterization, Vol. 4, p. 26-37.

[4] Laser Doppler Velocimetry. C. Gromke. TWEET-IE Grand Opening Event, Athens, Feb 2023: http://tweet-ie.ntua.gr/Uploads/20230124-26_GOE/TWEET-IE_GOE_Proceedings.zip

[5] B. Ruck (1990) Einfluß der Tracerteilchengröße auf die Signalinformation in der Laser-Doppler-Anemometrie, Technisches Messen, Vol. 57, p. 284-295.

[6] R.N. Meroney, M. Pavageau, S. Rafailidis, M. Schatzmann (1996) Study of line source characteristics for 2-D physical modelling of pollutant dispersion in street canyons, Journal of Wind Engineering and Industrial Aerodynamics, Vol. 62, p. 37-56.

[7] C. Gromke (2018) Wind tunnel model of the forest and its Reynolds number sensitivity, Journal of Wind Engineering and Industrial Aerodynamics, Vol. 175, p. 53-64.

[8] V. Pappa, D. Bouris, W. Theurer, C. Gromke (2023) A wind tunnel study of aerodynamic effects of façade and roof greening on air exchange from a cubic building. Building and Environment, Vol. 231, 110023.

[9] TSI, "INSIGHT 4G Manual,". https://www.scribd.com/document/378963876/INSIGHT4G-Software-Manual. accessed: 17.09.2023

[10] Building & Environmental Aerodynamics (LGU) of KIT (Karlsruhe Institute of Technology), personal communication

[11] M. Raffel, C. E. Willert, S. T. Wereley and J. Kompenhans, Particle Image Velocimetry: A Practical Guide, Heidelberg: Springer Berlin, 2007

[12] Keane, R. D., Adrian, R. J., Optimization of particle image velocimeters. I. Double pulsed systems, *Measurement science and technology* (1990) 1.11: 1202.

[13] Pappa, V., Manolesos, M., Langidis, A., Bouris, D., Stereo PIV measurements of vertical variation of local ventilation rates for a generic building exposed to an atmospheric boundary layer, in In Eleventh International Symposium on Turbulence and Shear Flow Phenomena (TSFP11) (2019).

[14] M. Manolesos, Experimental and computational study of three-dimensional separation and its control using passive vortex generators., PhD Thesis. National Technical University of Athens, 2014

[15] R. M. Waldman and S. B. Kenneth, "Accurate measurement of streamwise vortices using dual-plane PIV.," Experiments in fluids, no. 53: 1487-1500., 2012.

[16] TSI THERMAL ANEMOMETRY PROBES. tsi.com/getmedia/2e3fafd5-8037-40a9-aa38-4fa05a1d3ef3/Hotwire_Catalog_2980465?ext=.pdf. accessed: 17.09.2023.

[17] VDI 3783 Part 12, Environmental Meteorology Physical Modelling of Flow and Dispersion Processes in the Atmospheric Boundary Layer. Applications of Wind
Tunnels, Beuth Verlag, Berlin, 2000..

[18] Eurocode 1, Actions on structures - Part 1- 4: General actions - Wind actions. 1991, in: Authority: The European Union Per Regulation 305/2011, Directive 98/34/EC, Directive 2004/18/EC, 2005.

[19] I. P. Castro and A. G. Robins, "The flow around a surface-mounted cube in uniform and turbulent streams," Journal of fluid Mechanics, Vols. 79(2), 307-335, 1977.

[20] J. Westerweel and F. Scarano, "Universal outlier detection for PIV data," *Experiments in Fluids,* no. 39: 1096–1100, 2005.